This is a PDF file of the unedited manuscript that was accepted for publication:

Feasibility of using rural waste products to increase the denitrification efficiency in a surface flow constructed wetland.

Rosanna Margalef-Marti, Raúl Carrey, Daniel Merchán, Albert Soler, Jesús Causapé, Neus Otero

1 **Feasibility of using rural waste products to increase the denitrification efficiency in a**

2 **surface flow constructed wetland**

3 Rosanna Margalef-Marti[1], Raúl Carrey[1], Daniel Merchán[2], Albert Soler[1], Jesús Causapé[3], Neus

4 Otero[1,4]

5 [1] Grup MAiMA, SGR Mineralogia Aplicada, Geoquímica i Geomicrobiologia, Departament de

6 Mineralogia, Petrologia i Geologia Aplicada, SIMGEO UB-CSIC, Facultat de Ciències de la Terra,

7 Universitat de Barcelona (UB), C/Martí i Franquès s/n, 08028, Barcelona, Spain

8 [2] Department of Engineering, IS-FOOD Institute (Innovation & Sustainable Development in Food

9 Chain), Public University of Navarre, Campus de Arrosadia, 31006, Pamplona, Navarra, Spain

10 [3] Geological Survey of Spain—IGME, C/Manuel Lasala 44 9°B, 50006, Zaragoza, Spain

11 [4] Serra Húnter Fellowship, Generalitat de Catalunya, Spain.

12 **ABSTRACT**

13 A surface flow constructed wetland (CW) was set in the Lerma gully to decrease nitrate (NO_3^-)

14 pollution from agricultural runoff water. The water flow rate and NO_3^- concentration were

15 monitored at the inlet and the outlet, and sampling campaigns were performed which consisted

16 of collecting six water samples along the CW flow line. After two years of operation, the NO_3^-

17 attenuation was limited at a flow rate of ~2.5 L/s and became negligible at ~5.5 L/s. The present

18 work aimed to assess the feasibility of using rural waste products (wheat hay, corn stubble, and

19 animal compost) to induce denitrification in the CW, to assess the effect of temperature on this

20 process, and to trace the efficiency of the treatment by using isotopic tools. In the first stage,

21 microcosm experiments were performed. Afterwards, the selected waste material was applied in

22 the CW, and the treatment efficiency was evaluated by means of a chemical and isotopic

23 characterization and using the isotopic fractionation (ε) values calculated from laboratory

24 experiments to avoid field-scale interference. The microcosms results showed that the stubble

25 was the most appropriate material for application in the CW, but the denitrification rate was found

26 to decrease with temperature. In the CW, biostimulation in autumn-winter promoted NO_3^-

27 attenuation between two weeks and one month (a reduction in NO_3^- between 1.2 and 1.5 mM

28   was achieved). After the biostimulation in spring-summer, the attenuation was maintained for

29   approximately three months (NO_3^- reduction between 0.1 and 1.5 mM). The $\varepsilon^{15}N_{NO3/N2}$ and

30    $\varepsilon^{18}O_{NO3/N2}$ values obtained from the laboratory experiments allowed to estimate the induced

31   denitrification percentage. At an approximate average flow rate of 16 L/s, at least 60 % of NO_3^-

32   attenuation was achieved in the CW. The field samples exhibited a slope of 1.0 for $\delta^{18}O$-NO_3^-

33   versus $\delta^{15}N$-NO_3^-, similar to those of the laboratory experiments (0.9-1.2). Plant uptake seemed

34   to play a minor role in NO_3^- attenuation in the CW. Hence, the application of stubble in the CW

35   allowed the removal of large amounts of NO_3^- from the Lerma gully, especially when applied

36   during the warm months, but its efficacy was limited to a short time period (up to three months).

37   **Keywords**: denitrification, constructed wetland, electron donor, isotopic fractionation,

38   remediation.

39   **1. INTRODUCTION**

40   Since nitrate (NO_3^-) is known to cause ecological and human health problems (Vitousek et al.,

41   1997; Ward et al., 2005), the presence of this nutrient in water bodies worldwide is a matter of

42   concern. The extensive application of synthetic and organic fertilizers is a major source of NO_3^-

43   pollution. Therefore, agricultural runoff water should be treated before it is drained into larger

44   water bodies such as aquifers, rivers, and/or lakes. Constructed wetlands (CWs) are considered

45   promising, low cost systems for the remediation of diverse water pollutants, are simple to operate,

46   and have low energy requirements (Wu et al., 2015). Hence, directing agricultural runoff water

47   through a CW could be useful for removing NO_3^- to minimize pollution.

48   The surface flow CWs consists of free surface water flowing horizontally through an artificial pond

49   containing floating and/or emergent rooted vegetation and a high diversity of microorganisms

50   (Ilyas and Masih, 2017; Sirivedhin and Gray, 2006; Vymazal, 2007). The main processes that

51   might contribute to NO_3^- pollution mitigation in surface flow CWs are plant uptake, assimilation by

52   microorganisms, and denitrification (Rogers et al., 1991). The latter refers to the reduction of NO_3^-

53   by microorganisms through a series of enzymatic reactions involving the intermediates NO_2^-, NO,

54   and N_2O, before finally being reduced to N_2 (Knowles, 1982). Parameters such as temperature,

55   dissolved oxygen (O_2), NO_3^- loading, the source and amount of organic carbon (C), microbial

56   species, the type and density of macrophytes, wetland age, and hydraulic conditions play key

57   roles in the NO_3^- removal efficiency (Bachand and Horne, 1999; Beutel et al., 2009; Kong et al.,

58   2009; Sirivedhin and Gray, 2006). Different approaches can be implemented to enhance water

59   remediation, but strategies directed toward the induction of bacterial NO_3^- respiration are

60   preferred since denitrification is an authentic N sink in water, unlike biomass sequestration (Scott

61   et al., 2008). N storage by plants is generally considered temporary, because organic N returns

62   to the system after the death and decay of plants if they are not harvested (Cooper and Cooke,

63   1984; Gumbricht, 1993).

64   In CWs, macrophytes are able not only to assimilate NO_3^-, but also to promote denitrification

65   efficiency. Plants exert an influence on the diversity of microbial species and their enzymatic

66   activities by releasing exudates and oxygen to the rhizosphere (Kong et al., 2009, and references

67   therein), and decomposed plant material can be used by microbes as a source of organic C. For

68   this reason, increased NO_3^- removal is usually found in vegetated CWs relative to that in non-

69   vegetated systems (Jacobs and Harrison, 2014; Soana et al., 2017). If the CW cannot provide

70   enough organic C to support complete denitrification (e.g., from inlet water, soil, plant root

71   exudates, and decomposed vegetal material), the addition of an external organic C source as an

72   electron donor could enhance the heterotrophic denitrification efficiency (Lu et al., 2009; Si et al.,

73   2018). Since the use of pure reagents such as glucose, acetate, or ethanol may be expensive in

74   long-term treatments, the use of industrial or agricultural residues that are rich in organic C could

75   represent a more sustainable solution. Solid products such as animal or vegetal waste (Grau-

76   Martínez et al., 2017; Si et al., 2018; Trois et al., 2010), as well as industrial liquid by-products

77   (Carrey et al., 2018; Margalef-Marti et al., 2019), have already been reported as being useful for

78   promoting denitrification.

79   The pollutant removal efficiency in CWs can be estimated by monitoring the inlet and outlet

80   concentrations of the pollutant (Kovacic et al., 2000; Tanner et al., 2005; Uusheimo et al., 2018).

81   However, this method does not reveal the specific processes involved in the attenuation, making

82   it challenging to focus on the improvement of the wetland design and operation. Stable isotope

83   analyses can provide information on the NO_3^- transformation pathways. In the course of

84   denitrification, the unreacted residual NO_3^- becomes enriched in the heavy isotopes ^{15}N and ^{18}O,

85   permitting the distinction between biological attenuation and other processes such as dilution

86   which could also lead to decreases in concentration without influencing the isotopic signature

87   (Böttcher et al., 1990; Fukada et al., 2003; Mariotti et al., 1981; Aravena and Robertson, 1998).

88   In plants, significant enrichment in both ^{15}N and ^{18}O is observed in the NO_3^- extracted from leaves

89   after uptake relative to the NO_3^- from water, but the changes in the NO_3^- isotopic composition in

90   the water are minor (Estrada et al., 2017; Spoelstra et al., 2010). Therefore, the NO_3^- isotopic

91   characterization of water samples collected at the CW might improve the understanding and

92   support the evaluation of the performance of the remediation strategy.

93   In this context, the present work was developed to assess the feasibility of using rural waste

94   products (wheat hay, corn stubble, and animal compost) to induce denitrification in a surface flow

95   CW, and to trace the treatment efficiency in the autumn-winter and spring-summer seasons. In

96   the first stage, lab-scale experiments were performed to identify the most appropriate electron

97   donor to be applied in the CW, and to evaluate the effect of temperature on NO_3^- reduction. The

98   isotopic fractionations (ε) of N and O of dissolved NO_3^- under each condition were also

99   determined. In the second stage, the selected material was applied in the CW and the treatment

100   efficiency was evaluated by means of a chemical and isotopic characterization using the ε values

101   calculated from the laboratory experiments.

102   **2. METHODS**

103   *2.1. Laboratory experiments*

104   Six types of batch experiments were performed in 150 mL crystal Pyrex® bottles crimp-sealed

105   with butyl rubber stoppers under an argon (Ar) headspace. Each microcosm contained 100 mL

106   of water (2 mM NO_3^-) collected from the inlet of the studied CW (see Section 2.2) and a specific

107   C source: corn stubble (1 g); wheat hay (1 g); or animal compost (0.25 g). The six series of parallel

108   experiments were determined according to the waste product employed and the incubation

109   temperature. Series I (C-24) and II (H-24) contained animal compost and wheat hay, respectively,

110   and were incubated at 24 ºC; series III (S-24), IV (S-16), and V (S-8) contained corn stubble and

111   were incubated at 24 ºC, 16 ºC, and 8 ºC, respectively; series VI (DS-24) contained partially

112   decomposed corn stubble and was incubated at 24 ºC. The partially decomposed stubble was

113   obtained from the CW 7.5 months after its application on September 25, 2017 (see Section 2.2).

114   All series included at least eight replicates of the biostimulated microcosms. Control microcosms

115   for each tested material were prepared using deionized water (DIW) to discard the potential

4

116   supply of N from the waste products. The detailed content of each microcosm is described in

117   **Table 1**. During incubation, all microcosms were maintained in darkness and under constant

118   vibratory shaking. The biostimulated microcosms were sacrificed at time intervals depending on

119   the denitrification dynamics until complete NO_3^- and NO_2^- removals were achieved. The control

120   microcosms were sacrificed at the end of the biostimulation experiments. Water samples from

121   batch experiments were analyzed for major anions (NO_3^-, NO_2^-, Cl^-, and SO_4^{2-}), ammonium

122   (NH_4^+), non-purgeable dissolved organic C (NPDOC), dissolved inorganic C (DIC), major cations,

123   trace elements, $\delta^{15}N\text{-}NO_3^-$, $\delta^{18}O\text{-}NO_3^-$, and $\delta^{13}C\text{-}DIC$. Samples from control microcosms were

124   analyzed for major anions and NPDOC. The gas accumulated in the headspace of the vials was

125   collected and analyzed for nitrous oxide (N_2O) concentration. The three organic C sources were

126   analyzed for C and N concentrations and $\delta^{13}C\text{-}C_{bulk}$ and $\delta^{15}N\text{-}N_{bulk}$.

127   *2.2. CW test*

128   In the 2000s, approximately 20,000 ha of rainfed croplands were transformed into irrigated

129   agricultural land in the Arba River Basin (Zaragoza, Spain). A small watershed representative of

130   the area (Lerma basin, 733 ha) was monitored to assess the effects of this transformation on the

131   water balance and the salt and NO_3^--N exports (Merchán et al., 2015, 2014, 2013). In general,

132   the implementation of irrigation implied a three-fold increase in N export to the receiving water

133   bodies, in this case the Arba River, which was the first surface water body in the Ebro River Basin

134   to be declared affected by NO_3^- pollution according to the Nitrates Directive 91/676/EEC. In order

135   to diminish the release of NO_3^- from the Lerma Basin to the Arba River, a surface flow CW was

136   constructed in October 2015, initially covering an area of ~1500 m^2, and was enlarged in June

137   2017, covering a final area of ~2500 m^2 with a depth of ~40 cm. The surface water of the Lerma

138   gully can be partially diverted towards the CW. Water flow in the Lerma gully varies between 15

139   and 60 L/s. Temperature and precipitation data collected monthly in the area are reported in

140   Supporting information (**Table S1**).

141   The CW is fully automated, with high-frequency monitoring (every 10 minutes) of the water flow

142   rate and NO_3^- concentration at both the inlet and the outlet. Emergent macrophytes (*Typha* and

143   *Phragmites*) started growing since its construction, and occupied approximately 75 % of the CW

144   surface at the time the present study began, since the enlarged part was still unvegetated. The

145   field survey was performed in three periods and involved 13 sampling campaigns, each consisting

146   of the collection of six water samples (H1 to H6) from along the wetland flow line (**Figure 1**). In

147   the first period (June to September 2017), two different operating conditions were tested before

148   the biostimulation by modifying the inlet opening; three sampling campaigns were performed at

149   two different flow rates (~5.5 L/s and ~2.5 L/s). The second period involved the application of corn

150   stubble obtained from the surrounding crops (~8000 kg) on September 25, 2017, and the

151   evaluation of treatment efficiency by performing two sampling campaigns 7 and 14 d after the

152   application. The third period involved a second application of corn stubble (~6000 kg) on May 11,

153   2018, and the evaluation of treatment efficiency by performing eight sampling campaigns from

154   May 2018 to October 2018. In the two biostimulation periods, the corn stubble was applied over

155   all the CW surface between H1 and H3. Throughout these second and third periods, the CW was

156   operated at a higher flow rate (~16 L/s). The given flow rate for the CW test periods is that

157   measured at the outlet. The calculated residence time of NO_3^- in the CW was 21, 51 and 112 h

158   for the tested flow rates of 16, 5.5 and 2.5 L/s, respectively. Detailed information about the

159   sampling campaigns is shown in **Table 2**. Water samples collected at the CW were analyzed for

160   major anions (NO_3^-, NO_2^-, Cl^-, and SO_4^{2-}), NH_4^+, NPDOC, DIC, major cations, trace elements,

161    $\delta^{15}N\text{-}NO_3^-$, $\delta^{18}O\text{-}NO_3^-$, $\delta^{34}S\text{-}SO_4^{2-}$, $\delta^{18}O\text{-}SO_4^{2-}$, and $\delta^{13}C\text{-}DIC$.

162   *2.3. Analytical methods*

163   Water samples for the field and laboratory batch experiments were immediately filtered through

164   0.2 µm Millipore® filters after being collected, and were stored at 4 ºC until analysis. The aliquots

165   for NH_4^+, $\delta^{15}N\text{-}NO_3^-$, and $\delta^{18}O\text{-}NO_3^-$ analysis were frozen, and the aliquots for the DIC and $\delta^{13}C\text{-}$

166   DIC analyses were left with no headspace and stored at 4 ºC.

167   Anions (Cl^-, NO_2^-, NO_3^-, and SO_4^{2-}) were analyzed by high-performance liquid chromatography

168   (HPLC) (Waters 515 pump and Waters IC-Pak anion column with Waters 432 and KONTRON

169   UV/Vis detectors). NH_4^+ was analyzed by three techniques due to equipment availability issues:

170   I) spectrophotometry using the indophenol blue method (CARY 1E UV-visible), II) ion

171   chromatography or III) ammonia ion selective electrode (ORION, Thermo Scientific). DIC was

172   analyzed by titration (METROHM 702 SM Titrino), NPDOC by organic matter combustion (TOC

173   500 SHIMADZU), and major cations and trace elements by ICP-OES (Perkin Elmer Optima 8300).

174 The concentration of N_2O accumulated at the headspace of the vials was analyzed by gas

175 chromatography (GC) (Thermo Scientific Trace 1300 with ECD detector), and C and N

176 concentrations in the waste materials employed as C sources were analyzed with an elemental

177 analyzer (EA) (Carlo Erba1108 CHNS-O EA). The $\delta^{15}N\text{-}NO_3^-$ and $\delta^{18}O\text{-}NO_3^-$ were determined

178 following the cadmium and azide reduction method (McIlvin and Altabet, 2005; Ryabenko et al.,

179 2009). The isotopic composition of the N_2O obtained from the NO_3^- reduction was analyzed using

180 a Pre-Con coupled to a Finnigan MAT 253 isotope ratio mass spectrometer (IRMS) (Thermo

181 Scientific). For the SO_4^{2-} isotopic analysis, the dissolved SO_4^{2-} was precipitated as $BaSO_4$ by

182 adding $BaCl_2 \cdot 2H_2O$ after acidifying the sample with HCl and boiling it in order to prevent

183 precipitation of $BaCO_3$ (Dogramaci et al., 2001). The $\delta^{34}S\text{-}SO_4^{2-}$ was analyzed with a Carlo Erba

184 EA coupled in continuous flow to a Finnigan Delta XP Plus IRMS, whereas the $\delta^{18}O\text{-}SO_4^{2-}$ was

185 analyzed with a ThermoQuest high-temperature conversion analyzer (TC/EA) coupled in

186 continuous flow to a Finnigan Matt Delta XP Plus IRMS. The $\delta^{13}C\text{-}DIC$ was analyzed via

187 carbonate conversion to CO_2 gas by adding a phosphoric acid solution and measuring the gas

188 evolved with a Gas-Bench II coupled to a MAT-253 IRMS (Thermo Scientific). The $\delta^{13}C\text{-}C_{bulk}$ and

189 $\delta^{15}N\text{-}N_{bulk}$ of the waste materials employed as C sources were determined with a Carlo Erba EA

190 coupled to a Finnigan Delta C IRMS.

191 The isotopic notation is expressed in terms of δ (‰) relative to the international standards:

192 atmospheric N_2 (AIR) for $\delta^{15}N$, Vienna Standard Mean Oceanic Water (V-SMOW) for $\delta^{18}O$,

193 Vienna Pee Dee Belemnite (V-PDB) for $\delta^{13}C$, and Vienna Canyon Diablo Troillite (V-CDT) for

194 $\delta^{34}S$. Hence, $\delta = ((R_{sample} - R_{standard})/R_{standard})$, where R is the ratio between the heavy and the light

195 isotopes. Following Coplen (2011), several international and laboratory (CCiT) standards were

196 interspersed among the samples for normalization of the results (Supporting Information **Table**

197 **S2**). The reproducibilities (1 σ) of the samples, calculated from the standards systematically

198 interspersed in the analytical batches, were ±1.0 ‰ for $\delta^{15}N\text{-}NO_3^-$, ±1.5 ‰ for $\delta^{18}O\text{-}NO_3^-$, ±0.2 ‰

199 for $\delta^{15}N\text{-}N_{bulk}$, ±0.2 ‰ for $\delta^{13}C\text{-}C_{bulk}$, ±0.2 ‰ for $\delta^{13}C\text{-}DIC$, ±0.2 ‰ for $\delta^{34}S\text{-}SO_4^{2-}$, and ±0.5 ‰ for

200 $\delta^{18}O\text{-}SO_4^{2-}$. Samples for chemical and isotopic analyses were prepared at the laboratory of the

201 MAiMA-UB research group, and analyzed at the Centres Científics i Tecnològics of the Universitat

202 de Barcelona (CCiT-UB).

203 **3. RESULTS AND DISCUSSION**

204   *3.1. Lab-scale evaluation of the nitrate removal capacities of compost, hay, and stubble at 24 ºC*

205   The chemical and isotopic characterization of the samples obtained from the laboratory

206   experiments are presented in the Supporting Information (**Table S3**). Although the intrinsic N

207   content measured in the three waste products (stubble, hay, and compost) were low (**Table 3**), it

208   was not possible to disregard a certain supply of N from these materials throughout the

209   incubations. The control microcosms containing the three C sources and DIW showed NO_3^-, NO_2^-

210   , and NH_4^+ concentrations below 0.09 mM, 0.02 mM, and 0.12 mM, respectively.

211   The biostimulation experiments showed that the three tested C sources were able to promote

212   NO_3^- removal. Complete denitrification (total NO_3^- and NO_2^- removal) was reached in

213   approximately 40 h in the microcosms containing stubble and hay, and in approximately 95 h in

214   that containing compost (**Figure 2A**). NH_4^+ was detected in some of the samples (in

215   concentrations of up to 1 mM), but with no clear pattern, suggesting the possible coexistence of

216   denitrification and dissimilatory NO_3^- reduction to NH_4^+ (DNRA) and/or the input of NH_4^+-N

217   supplied from the C sources tested. Transient NO_2^- accumulation of up to 1.5 mM (stubble and

218   hay) and 0.7 mM (compost) were observed. The highest concentration of NO_2^- in the stubble and

219   hay microcosms were detected after complete NO_3^- reduction, and subsequently decreased to

220   below the detectable limit in less than 40 h from the beginning of the experiment. Contrarily, in

221   the microcosms containing compost, the highest NO_2^- concentration was observed after 40 h,

222   and thereafter decreased along with NO_3^- concentration until both compounds were below the

223   detectable limits, after 96 h. The differences in NO_2^- accumulation between the compost, stubble,

224   and hay experiments were likely related to the rate of NO_3^- reduction. NO_2^- accumulation has

225   been reported to depend on the relative rates of NO_3^- and NO_2^- reduction (Betlach and Tiedje,

226   1981), as well as on the type of C source and C/N ratios employed (Akunna et al., 1993; Ge et

227   al., 2012). The slower reduction observed with compost could be due to the lower amount of

228   material used in the experiments (0.25 g instead of the 1 g used for stubble and hay). Although

229   the intrinsic C concentrations of the three sources were similar (**Table 3**), the C bioavailability

230   could differ between each product, and even between replicates, due to heterogeneity in the

231   materials (Breulmann et al., 2014; Sobczak and Findlay, 2002; Warneke et al., 2011).

232   Consequently, the NPDOC concentration did not show a clear correlation with NO_3^- reduction,

233   but provided an approximation of the amount of added C present in dissolved form. Although the

8

234 quantity of compost in the microcosms was only one-quarter of the quantity of vegetal materials

235 used, the measured NPDOC concentrations in the three types of microcosms were similar (13.2-

236 27.3 mM for stubble, 11.8-16.8 mM for hay, and 5.3-14.3 mM for compost). The δ^{13}C-DIC

237 provided information about the transformation of organic C from the waste materials to inorganic

238 C; a brief discussion is presented in the Supporting Information (**section S1**).

239 Concerning the safety of the materials, the ICP-OES analyses showed that there was no release

240 of toxic trace elements from any of the tested compounds (Supporting Information **Table S4**). Hay

241 and stubble seemed to be more feasible than compost for application in the CW. Compost

242 resulted in a lower denitrification rate, the NO_2^- accumulation lasted longer, and it was highly

243 soluble and could be rapidly removed from the CW via the water flow. In this study, stubble was

244 selected for application in the studied CW due to a higher availability in the area. Therefore, further

245 experiments were only performed with stubble.

246 *3.2. Lab-scale evaluation of the effect of temperature on denitrification induction by stubble*

247 The denitrification activity of microorganisms is usually increased with higher temperatures, and

248 therefore higher NO_3^- attenuation from water can be observed during warm periods (Rivett et al.,

249 2008; Spieles and Mitsch, 1999). To assess the effect of temperature on the induced

250 denitrification strategy, additional experiments were performed. A comparison between different

251 incubation temperatures in corn stubble experiments showed that denitrification reached

252 completion across the whole temperature range studied (from 8 to 24 ºC), but with different lag

253 periods and NO_3^- reduction rates. Complete denitrification was achieved after 40 h at 24 ºC, 65 h

254 at 16 ºC, and 140 h at 8 ºC (**Figure 2B**). The decrease in NO_3^- began after 10 h at 24 ºC, whereas

255 at 16 ºC and 8 ºC lag periods of 45 h and 79 h, respectively, were observed. A decrease in NO_3^-

256 reduction rate associated with lower temperatures following the Arrhenius relationship has been

257 well documented (Dawson and Murphy, 1972). Therefore, the denitrification efficiency might

258 decrease during the winter months or low-temperature periods in comparison to that during the

259 summer months, and thus application of the carbon source throughout the spring months might

260 be advantageous. Significant transient NO_2^- accumulation (up to 1.5 mM at 24 ºC, 1.8 mM at 16

261 ºC, and 1.0 mM at 8 ºC) was observed in all the experiments. As discussed in the previous section,

262 NO_2^- accumulation was less significant in the experiment with a lower denitrification rate (8 ºC).

263 *3.3. Lab-scale assessment of the lifespan of the denitrification induced by stubble*

264 One of the main issues associated with biostimulation strategies is their effectiveness during long-

265 term treatments. It is thus important to consider the lifespan of the material to be employed in the

266 CW. In another laboratory experiment with vegetable materials (palm leaves and compost),

267 induced NO_3^- degradation was shown to be maintained for more than 220 d (Grau-Martínez et

268 al., 2017). In this context, microcosms containing partially decomposed stubble (sampled in the

269 CW 7.5 months after its application) were incubated and compared to microcosms containing

270 fresh stubble. The denitrification induced by the partially decomposed stubble proceeded at a

271 higher rate than that induced by the fresh stubble; complete NO_3^- reduction was achieved in less

272 than 25 h with the former, instead of 40 h with the latter (**Figure 2B**). In the partially decomposed

273 stubble microcosms, transient NO_2^- accumulation was below 0.8 mM. Due to the increased

274 heterogeneity of the material after being in the field and in contact with water for months, high

275 variabilities in both NO_3^- and NO_2^- concentrations were observed between replicates. Therefore,

276 the reduction rates obtained from these experiments must be considered approximations. These

277 results showed that the intrinsic capacity of the stubble to promote denitrification after 7.5 months

278 being in contact with water was still important, at least at lab-scale. However, the NPDOC content

279 in the microcosms containing partially decomposed stubble (1.7-8.8 mM) were lower than those

280 in the microcosms with fresh stubble incubated at 24 ºC (13.2-27.3 mM), pointing to a decreased

281 availability of the electron donor over time. In the CW, the specific lifespan of the treatment might

282 be shorter, since the organic C also typically consumes O_2 before using NO_3^- as an electron

283 donor. The N_2O accumulated in the headspace of the microcosms containing partially

284 decomposed stubble incubated at 24 ºC (as well as that in the microcosms containing fresh

285 stubble incubated at 16 and 8 ºC) was also measured since the release of greenhouse gases

286 during N transformation processes is a matter of concern. The maximum N_2O concentration

287 detected accounted for 0.015 % of the initial $N-NO_3^-$ content of the microcosms (Supporting

288 Information (**Table S3**)).

289 *3.4. Lab-scale: NO_3^- isotopic fractionation calculation.*

290 Under closed-system conditions, the isotopic fractionation (ε) for a determined element (e.g., N

291 and O from dissolved NO_3^-) can be calculated by means of a Rayleigh distillation equation

292   (**Equation 1**). Thus, ε can be obtained from the slope of the linear correlation between the natural

293   logarithm of the remaining substrate fraction (Ln($C_{residual}/C_{initial}$), where C refers to analyte

294   concentration) and the determined isotope ratios (Ln($R_{residual}/R_{initial}$), where R = δ+1). These

295    $\varepsilon^{15}N_{NO3/N2}$ and $\varepsilon^{18}O_{NO3/N2}$ values, determined at lab-scale under controlled conditions, can be later

296   applied at field-scale to estimate the contribution of denitrification to the NO_3^- attenuation, while

297   avoiding field-scale interference such as dilution due to rainfall (Böttcher et al., 1990; Mariotti et

298   al., 1988). We calculated $\varepsilon^{15}N_{NO3/N2}$ and $\varepsilon^{18}O_{NO3/N2}$ under all tested conditions at lab-scale (**Figure**

299   **3**) to appropriately evaluate the efficacy of the induced denitrification strategy tested at the CW.

300   A summary of the calculated $\varepsilon^{15}N_{NO3/N2}$, $\varepsilon^{18}O_{NO3/N2}$, and $\varepsilon^{15}N/\varepsilon^{18}O$ values is shown in (**Table 4**);

301    $\varepsilon^{15}N_{NO3/N2}$ ranged from -31.9 to -10.5‰, $\varepsilon^{18}O_{NO3/N2}$ from -30.4 to -9.7‰, and $\varepsilon^{15}N/\varepsilon^{18}O$ from 0.8 to

302   1.8. These values fall within the reported range for heterotrophic denitrification (see Table 4;Grau-

303   Martínez et al., (2017)). The lowest $\varepsilon^{15}N_{NO3/N2}$ and $\varepsilon^{18}O_{NO3/N2}$ values were found for the

304   microcosms containing compost incubated at 24 ºC and stubble incubated at 8 ºC, which were

305   the two experiments that presented lower NO_3^- reduction rates. Apart from the microcosms

306   containing stubble incubated at 8 ºC, the other microcosms containing stubble (both fresh and

307   partially decomposed and incubated at 16 or 24 ºC) presented narrower ranges of $\varepsilon^{15}N_{NO3/N2}$ (from

308   -28.3 to -22.5‰), $\varepsilon^{18}O_{NO3/N2}$ (from -30.4 to -21.2‰) and $\varepsilon^{15}N/\varepsilon^{18}O$ (from 0.8 to 1.1). These values

309   were employed to assess the efficiency of the biostimulation strategy at the studied CW.

310    $$Ln\left(\frac{R_{residual}}{R_{initial}}\right) = \varepsilon \times Ln\left(\frac{C_{residual}}{C_{initial}}\right)$$ **Equation 1**

311   *3.5. Performance of the CW before application of stubble*

312   The chemical and isotopic characterization of the samples obtained from the CW both before and

313   after application of the electron donor are presented in Supporting Information (**Table S5**). Three

314   sampling campaigns were performed at the CW before stubble application. While NO_3^- was not

315   significantly reduced during the two sampling campaigns performed at a ~5.5 L/s flow rate (June

316   and September 2017), a slight attenuation (from 1.3 to 0.8 mM) occurred under operation at ~2.5

317   L/s (September 2017) (**Figure 4A**). In all samples, NO_2^- was below the detection limit and NH_4^+

318   was below 0.01 mM, suggesting that NO_3^- had been either transformed to gaseous N products

319   through denitrification or assimilated by plants or microorganisms (Supporting information (**Table**

320   **S5)**). Whereas no increase in $\delta^{15}N$-NO_3^- nor $\delta^{18}O$-NO_3^- was observed in the samples collected

321 during the first campaign at ~5.5 L/s (June 14, 2017), an increase was observed at the middle

322 section of the CW (H3) during the second survey at ~5.5 L/s (September 5, 2017). In this latter

323 campaign, the inlet (H1) presented $\delta^{15}N\text{-}NO_3^-$ and $\delta^{18}O\text{-}NO_3^-$ values of +11.6 ‰ and +8.7 ‰,

324 respectively, which increased at the middle point (H3) up to +19.2 ‰ and +18.2 ‰, respectively,

325 and decreased at the outlet (H6) to +9.6 ‰ and +7.1 ‰, respectively (**Figure 4B**). A proposed

326 explanation is that the occurrence of preferential flows within the wetland (e.g., heterogeneous

327 flow rate between surface and bottom water or between lateral and central water) could have led

328 to an increased hydraulic retention time and/or stagnant water at the H3 sampling site. In the

329 campaign performed at a ~2.5 L/s flow rate (September 12, 2017), the decrease in NO_3^-

330 concentration was coupled to increases in $\delta^{15}N\text{-}NO_3^-$ and $\delta^{18}O\text{-}NO_3^-$ from the inlet (+7.0 ‰ and

331 +4.7 ‰, respectively, at H1) to the outlet (+17.1 ‰ and +13.0 ‰, respectively, at H6) of the CW

332 (**Figure 4B**). The slope of the relation between $\delta^{18}O\text{-}NO_3^-$ and $\delta^{15}N\text{-}NO_3^-$ for the samples

333 collected in these three campaigns was 0.8 (r^2 = 0.91) (**Figure 4B**), which is indicative of

334 denitrification activity (Aravena et al., 1998). These results are in agreement with previous results

335 reporting the occurrence of denitrification in CWs even in the presence of dissolved O_2 (Sirivedhin

336 and Gray, 2006). The intrinsic denitrification activity in the CW did not support complete

337 denitrification, likely due to the low NPDOC content of the water (0.4 – 0.6 mM). Therefore, it was

338 decided to evaluate the feasibility of adding an external electron donor source to promote NO_3^-

339 attenuation when operating at a ~16 L/s flow rate.

340 *3.6. Performance of the CW after application of stubble*

341 Application of stubble in autumn (September 25, 2017) induced denitrification in the CW

342 approximately 2 d after the application (**Figure 5B**). Denitrification was almost complete at the

343 outlet (H6) by 14 d following the application (0.2 mM NO_3^- remaining of the initial 1.4 – 1.7 mM)

344 (**Figure 5A**). In the two sampling campaigns, NO_2^- accumulated beginning at H2 and reached a

345 concentration of 0.2 mM by the outlet (H6) by 7 d after treatment, but decreased to 0.1 mM by 14

346 d. Such a decrease in NO_2^- accumulation over time has been previously observed in laboratory

347 experiments and other denitrification studies (Carrey et al., 2014; Margalef-Marti et al., 2019;

348 Vidal-Gavilan et al., 2013). The maximum NH_4^+ concentration of 0.02 mM was measured at H3

349 after 7 d, while it decreased by the outlet (H6) to 0.01 mM in both campaigns, pointing to a non-

350 significant contribution of DNRA. Due to the application of stubble, the outlet flow rate decreased

351   until the system became partially blocked, leaving the monitoring probes exposed to the air. When

352   the problem was solved (October 17, 2017) and the outlet flow was stabilized at approximately

353   16 L/s, the NO_3^- concentration monitored at the outlet showed fluctuations, pointing to a slight

354   denitrification activity until October 24, 2017 (**Figure 5C**). Thus, the lifetime of the treatment in

355   autumn (recorded temperatures in October 2017 ranged from 10.3 ºC to 20.4 ºC, averaging 16.0

356   ºC) was estimated to be between 2 weeks and 1 month.

357   Application of stubble in spring (May 5, 2018) also induced denitrification and underwent a shorter

358   acclimation time (1 d) with respect to the first application, likely due to faster acclimation by the

359   previously stimulated bacterial community (**Figure 6A**). By 7 d after the stubble application, the

360   NO_3^- concentration at the outlet (H6) was 0.2 mM, and denitrification was complete after 14 d.

361   The NO_3^- concentration in the outlet then began to increase progressively until reaching a level

362   similar to that at the inlet by approximately 100 d after treatment (**Figure 6B**). A lower NO_3^-

363   concentration measured in H3 during the last sampling campaign (+161 d) was attributed to

364   stagnant water near the sampling point due to the accumulation of partially decomposed stubble.

365   Thus, the treatment in spring-summer (temperatures recorded from May to October 2018

366   presented monthly minimums from 9.6 to 19.9 ºC, monthly maximums from 20.0 to 28.4 ºC, and

367   monthly averages from 15.8 to 24.6 ºC) induced significant denitrification for approximately three

368   months, which is three times longer than that induced by the treatment in autumn. The NO_3^-

369   concentration decrease at the outlet compared to inlet during these three months ranged from 0.1

370   to 1.5 mM (highest attenuation corresponded to the first month after stubble application). All the

371   monitored NO_3^- concentrations at the inlet and outlet of the CW during this study period are

372   presented in the Supporting Information **Figure S1**. The increased efficiency of the treatment in

373   spring-summer compared to that of the treatment in autumn is in accordance with laboratory

374   results (incubation at 8, 16, and 24 ºC) and with previous wetland studies reporting increased

375   denitrification rates at higher temperatures (Bachand and Horne, 1999; Christensen and Srensen,

376   1986; Si et al., 2018). The faster acclimation by the previously stimulated bacterial community

377   could have been also responsible for this increased attenuation activity.

378   After the second stubble application, 0.1 mM of NO_2^- was detected at the outlet (H6) for 63 d.

379   Afterwards, it was no longer detected (except at the aforementioned point H3 where water

380   stagnated), confirming a decreased NO_2^- accumulation with time as observed during the previous

381   treatment period. The maximum NH_4^+ concentration detected, 0.3 mM, was recorded at H4 7 d

382   after application, while at the outlet (H6), the concentration was 0.05 mM. At 14 d and one month

383   after application, NH_4^+ at the outlet decreased to 0.02 mM and 0.01 mM, respectively. These

384   results suggest that transient DNRA activity could have arisen between H2 and H4 following the

385   stubble application. NO_3^- is reduced to NH_4^+ through DNRA, depending on parameters such as

386   microbial growth rate, NO_2^- accumulation, and the C:N ratio (Kraft et al., 2014). It is generally

387   accepted that DNRA is favored at high C:N ratios, when NO_3^- is limited (rather than the electron

388   donor being limited), or when high NO_3^- levels inhibit NO_2^- reductase (Giles et al., 2012; Kelso et

389   al., 1997). This hypothesis is consistent with the higher degree of NH_4^+ accumulation observed

390   in laboratory experiments compared to that observed in the field, since higher C:N ratios with a

391   more homogeneous distribution were found in the batch experiments. It is also necessary to

392   account for the possible input of N from the applied stubble. NO_2^- and NH_4^+ have a lower threshold

393   for human consumption (0.01 and 0.03 mM, respectively) with respect to that of NO_3^- (0.8 mM)

394   (98/83/EC, 1998). However, since NH_4^+ accumulation decreased before the outlet and fell to

395   insignificant levels by 14 d after treatment, and the NO_2^- accumulation also decreased over time,

396   stubble was considered effective in removing N compounds from agricultural runoff water.

397   A few authors have previously attempted to calculate the denitrification efficiency in CWs by

398   means of isotopic assessment, but using ε values available in the literature and only for $N-NO_3^-$

399   (Lund et al., 1999; Søvik and Mørkved, 2008). The $\varepsilon^{15}N_{NO3/N2}$ and $\varepsilon^{18}O_{NO3/N2}$ values obtained from

400   our lab-scale experiments in which fresh stubble was incubated at 24 and 16 ºC, and partially

401   decomposed stubble was incubated at 24 ºC, were used to calculate three denitrification % lines

402   (**Equation 2**, derived from **Equation 1**) that were plotted on a graph of $\delta^{18}O-NO_3^-$ versus $\delta^{15}N-$

403   NO_3^- along with the isotopic results for the CW samples (**Figure 7**). These three laboratory

404   conditions encompass the average temperatures recorded during the biostimulation periods

405   tested at the CW. The slope of $\delta^{18}O-NO_3^-$ versus $\delta^{15}N-NO_3^-$ for the field samples collected after

406   the biostimulation treatment was 1.0 (r^2 = 0.98) (**Figure 7**), which is slightly higher than that

407   obtained for the intrinsic denitrification before the stubble addition (0.8 (r^2 = 0.91)), which is likely

408   due to the use of a different C source and the promotion of a different bacterial community. Also,

409   the slope obtained after the biostimulation (1.0) was similar to the slopes obtained in the lab-scale

410   experiments using partially decomposed stubble incubated at 24 ºC (0.9) and those using fresh

411 stubble incubated at 24 and 16 °C (1.25 and 1.1, respectively). This is consistent with the

412 temperatures registered in the area throughout the test period, and with the stubble being in

413 contact with water. This similarity between the field-scale and lab-scale slopes, together with the

414 observed isotopic fractionation in the CW suggested that plant uptake did not likely contribute

415 significantly to the NO_3^- removal.

416 Denitrification % = $\left[1 - \left(\frac{C_{residual}}{C_{initial}} \right) \right]$ × 100 = $\left[1 - e^{\left(\frac{\delta_{residual} - \delta_{initial}}{\varepsilon} \right)} \right]$ × 100

417 **Equation 2**

418 The results showed that at least 60% of NO_3^- attenuation was achieved in the CW due to the

419 induced denitrification, although this value was obtained from the less-favorable situation (where

420 the denitrification % was calculated from the experiments using stubble incubated at 24 °C). If the

421 denitrification % is instead calculated based on the experiment using partially decomposed

422 stubble incubated at 24 °C, which presents the slope most similar to that of the field samples (0.9

423 compared to 1.0), then denitrification accounted for a 70 % NO_3^- removal. The largest contribution

424 of denitrification, as determined by isotopic data, was observed in the outlet samples (H6) taken

425 7 and 14 d after the first stubble application, and 7 d after the second stubble application. By 14

426 d after the second stubble application, NO_3^- concentration in some samples was below the level

427 required for the isotopic analysis. Therefore, the induced denitrification allowed a NO_3^- attenuation

428 close to 100 %. After two weeks of treatment, the contribution of the induced denitrification at the

429 outlet (H6) began to decrease, from 30 % in June 2018 to 5 % in September 2018, and slightly

430 increased to 20 % by the last survey in October 2018. Considering an average flow rate of 16 L/s

431 (the application of stubble led to fluctuations in the flow rate due to partial blockages at some

432 points caused by stubble accumulation) and these results, in the studied CW, at least 80 kg of

433 NO_3^- were removed per day over the first two weeks after the stubble application in May 2018

434 and 30 kg/d were removed from 14 to 63 d after the supply, after which time the removal

435 decreased. A comparison between the denitrification percentages calculated using chemical and

436 isotopic data revealed that using concentration values always resulted in a higher value. Since

437 the contribution calculated from the isotopic data was considered to be linked to NO_3^- attenuation

438 due to denitrification, the difference could be due to a decrease in NO_3^- concentration provoked

439 by dilution due to precipitation, or the contribution of plant uptake to NO_3^- attenuation.

3.7. Effect and evolution of NPDOC in the CW

441	Since the amount of organic C released from the CW to the Lerma gully, and from there to the

442	Arba River was a matter of concern, the NPDOC concentration in the field samples were

443	measured. Only the results obtained from the second stubble application are discussed (the first

444	application gave similar results). The NPDOC concentration at the outlet increased with respect

445	to the background values by 7 d after application, and the increased level was maintained for 14

446	d in total (**Figure 8**). The increase began at H3, reached a maximum between H4 and H5 (1.6 –

447	1.7 mM), and decreased to approximately 1.0 – 1.1 mM by the outlet (H6), indicating a release of

448	organic C to the gully (background NPDOC concentrations ranged from 0.5 to 0.8 mM). Because

449	the gully contained NO_3^--polluted water, it was considered that the surplus organic C could lead

450	to NO_3^- attenuation downstream. The high NPDOC concentration detected between H3 and H5

451	could have provoked a decrease in water quality within the CW due to the promotion of processes

452	such as DNRA (previously discussed) and bacterial SO_4^{2-} reduction (BSR), through which NH_4^+

453	and H_2S are produced, respectively. Although BSR is usually induced when NO_3^- is completely

454	removed from the environment, the coexistence of denitrification and BSR in the presence of an

455	abundance of an electron donor has also been demonstrated (Laverman et al., 2012). The

456	isotopic characterization of SO_4^{2-} can provide information to assess its transformation processes

457	because the decrease in SO_4^{2-} concentration is coupled to increases in $\delta^{34}S$-SO_4^{2-} and $\delta^{18}O$-

458	SO_4^{2-} through the BSR (Strebel et al., 1990). Correlation between SO_4^{2-} concentration and

459	isotopic composition was not identified in the samples collected at the CW, suggesting that BSR

460	was not occurring in the CW. Therefore, the possibility of a decrease in water quality in the CW

461	due to H_2S production as a result of excess organic C was discarded.

462	*3.8. Suitability of the strategy and future improvements*

463	The remediation strategy tested in the CW allowed the induction of the removal of NO_3^- from

464	agricultural runoff water. The NO_3^- attenuation was primarily related to denitrification. Previous

465	studies also found that denitrification was an important N sink in CWs in comparison to plant

466	uptake (Lin et al., 2002; Soana et al., 2017). It has to be considered that denitrification can only

467	be considered a N sink if intermediate products such as NO_2^- or N_2O are not accumulated during

468	the NO_3^- reduction. The added stubble could have enhanced denitrification not only by increasing

469   the organic C content of the water but also by inhibiting O_2 production through photosynthesis by

470   shading the water column, as previously hypothesized by Jacobs and Harrison (2014) for floating

471   vegetation in CWs. However, the denitrification efficiency was limited. The most likely explanation

472   involves the high O_2 content of the inlet water (near saturation, approximately 0.28 and 0.34 mM

473   in summer and winter, respectively) (Merchán et al., 2014) and the vast surface available for O_2

474   diffusion. Other parameters that could have also contributed to the limited denitrification efficiency

475   include the high water flow rate tested in the CW (~16 L/s), and the possible generation of

476   preferential flows within the CW (e.g., due to stubble accumulation in some points) that could led

477   to a low degree of interaction between water and stubble.

478   Although application of solid residues such as maize stubble in surface flow CWs might have

479   advantages over the application of liquid organic C sources, which face the problems of greater

480   loss by bacterial oxidation (Lin, 2002) and greater release with the water flow, new strategies for

481   increasing the lifespan and efficacy of the induced denitrification must be investigated. In addition,

482   increased intrinsic denitrification capacity of the CW is expected after plant growth covers the

483   entire surface. Previous studies have reported increased denitrification activity in vegetated CWs

484   relative to the levels in non-vegetated systems (Lin et al., 2002; Soana et al., 2017), with efficacy

485   varying among plants of different species or age (Lin et al., 2002; Lund et al., 1999). The organic

486   C pool released after plant senescence has also been demonstrated to increase the bacterial

487   activity, as this C can also be used as electron donor (Peralta et al., 2012; Soana et al., 2017). In

488   this direction, Kang et al. (2018) proposed the use of plants whose growth season is winter.

489   Therefore, the organic C supply from senescence would occur throughout the summer months,

490   when temperatures are higher and more appropriate conditions are established for the promotion

491   of significant denitrification activity.

492   N_2O production was not assessed in our field-scale tests. At lab-scale, limited N_2O production

493   was observed. However, at field-scale, higher N_2O emissions could occur as a result of

494   denitrification induced by the stubble addition because the high O_2 content of the inlet water and

495   the free surface water flow might allow more extensive O_2 diffusion in water. Since N_2O emissions

496   are detrimental for air quality, the production of this greenhouse gas should also be monitored in

497   treatments aiming to induce denitrification. Isotopic characterization of the N_2O emitted from a

498   given CW could also provide further information about the N transformation processes that led to

499   the decrease in NO_3^- concentration.

500   **4. CONCLUSIONS**

501   At laboratory-scale, maize stubble, wheat hay, and animal compost were able to induce complete

502   denitrification. Stubble was selected for field-scale application due to its better local availability.

503   In the following incubations, stubble sampled from the CW 7.5 months after its application was

504   still able to support complete NO_3^- attenuation. Complete NO_3^- attenuation was achieved over

505   the temperature range of 8 to 24 ºC, although lower temperatures resulted in lower reduction

506   rates. The $\varepsilon^{15}N_{NO3/N2}$ and $\varepsilon^{18}O_{NO3/N2}$ values obtained from the laboratory experiments allowed

507   evaluation of the performance of the remediation strategy at the CW.

508   Before the application of the stubble, NO_3^- attenuation at the CW (from 1.3 to 0.8 mM) was only

509   observed when the flow was decreased from approximately 5.5 to 2.5 L/s. The biostimulation in

510   autumn-winter promoted NO_3^- attenuation lasting between 2 weeks and one month, while in

511   spring-summer the attenuation capacity remained for approximately three months (~16 L/s flow

512   rate). The isotopic characterization of the CW samples indicated that at least 60 % of the initial

513   NO_3^- was removed in the CW due to the induced denitrification. However, since in a few samples

514   NO_3^- was below the limit necessary for isotopic analysis, the contribution could have been higher.

515   The slope of $\delta^{18}O$-NO_3^- versus $\delta^{15}N$-NO_3^- obtained in the CW after the stubble application (1.0)

516   was close to that obtained in the experiments involving partially decomposed stubble incubated

517   at 24ºC (1.1). Plant uptake seemed to play only a minor role in NO_3^- attenuation in the CW. The

518   treatment was considered safe because NO_2^- and NH_4^+ accumulation (below 0.2 and 0.1 mM,

519   respectively) decreased over time, surplus NPDOC (below 2.3 mM) released from the CW could

520   maintain NO_3^- attenuation downstream, and because the occurrence of BSR was discarded.

521   However, the longevity and effectivity of the treatment were limited due to the high O_2 content of

522   the inlet water, high water flow, and the possible generation of preferential flows within the CW.

REFERENCES

532   91/676/EEC, 1991. Nitrates Directive. Council Directive 91/676/EEC of 12 December 1991,

533   concerning the protection of waters against pollution caused by nitrates from agricultural

534   sources. [WWW Document]. Off. J. Eur. Comm. URL

535   http://ec.europa.eu/environment/index_en.htm (accessed 4.9.17).

536   98/83/EC, 1998. Drinking Water Directive. Council Directive 98/83/EC, of 3 November 1998, on

537   the quality of water intended for human consumption. [WWW Document]. Off. J. Eur.

538   Comm. URL http://ec.europa.eu/environment/index_en.htm (accessed 4.9.17).

539   Akunna, J.C., Bizeau, C., Moletta, R., 1993. Nitrate and nitrite reductions with anaerobic sludge

540   using various carbon sources: Glucose, glycerol, acetic acid, lactic acid and methanol.

541   Water Res. 27, 1303–1312. https://doi.org/10.1016/0043-1354(93)90217-6

542   Aravena, R., Robertson, W.D., 1998. Use of multiple isotope tracers to evaluate denitrification in

543   ground water: study of nitrate from a large-flux septic system plume. Ground Water 36,

544   975–982.

545   Bachand, P.A.M., Horne, A.J., 1999. Denitrification in constructed free-water surface wetlands:

546   I. Very high nitrate removal rates in a macrocosm study. Ecol. Eng. 14, 9–15.

547   https://doi.org/10.1016/S0925-8574(99)00016-6

548   Betlach, M.R., Tiedje, J.M., 1981. Kinetic Explanation for Accumulation of Nitrite, Nitric Oxide,

549   and Nitrous Oxide during Bacterial Denitrification. Appl. Environ. Microbiol. 42, 1074–

550   1084. https://doi.org/Article

551   Beutel, M.W., Newton, C.D., Brouillard, E.S., Watts, R.J., 2009. Nitrate removal in surface-flow

552   constructed wetlands treating dilute agricultural runoff in the lower Yakima Basin,

553   Washington. Ecol. Eng. 35, 1538–1546. https://doi.org/10.1016/j.ecoleng.2009.07.005

554   Böttcher, J., Strebel, O., Voerkelius, S., Schmidt, H.L., 1990. Using isotope fractionation of

555   nitrate-nitrogen and nitrate-oxygen for evaluation of microbial denitrification in a sandy

556   aquifer. J. Hydrol. 114, 413–424. https://doi.org/10.1016/0022-1694(90)90068-9

557   Breulmann, M., Masyutenko, N.P., Kogut, B.M., Schroll, R., Dörfler, U., Buscot, F., Schulz, E.,

558   2014. Short-term bioavailability of carbon in soil organic matter fractions of different

559   particle sizes and densities in grassland ecosystems. Sci. Total Environ. 497–498, 29–37.

560   https://doi.org/10.1016/j.scitotenv.2014.07.080

561   Carrey, R., Otero, N., Vidal-Gavilan, G., Ayora, C., Soler, A., Gómez-Alday, J.J., 2014. Induced

562   nitrate attenuation by glucose in groundwater: Flow-through experiment. Chem. Geol. 370,

563   19–28. https://doi.org/10.1016/j.chemgeo.2014.01.016

564   Carrey, R., Rodríguez-Escales, P., Soler, A., Otero, N., 2018. Tracing the role of endogenous

565   carbon in denitrification using wine industry by-product as an external electron donor:

566   Coupling isotopic tools with mathematical modeling. J. Environ. Manage. 207, 105–115.

567   https://doi.org/10.1016/j.jenvman.2017.10.063

568   Christensen, P.B., Srensen, J.A.N., 1986. Temporal Variation of Denitrification Activity in Plant-

569   Covered , Littoral Sediment from Lake Hampen , Denmark 51, 1174–1179.

570   Cooper, A.B., Cooke, J.G., 1984. Nitrate loss and transformation in 2 vegetated headwater

571   streams. New Zeal. J. Mar. Freshw. Res. 18, 441–450.

572   https://doi.org/10.1080/00288330.1984.9516065

573   Coplen, T.B., 2011. Guidelines and recommended terms for expression of stable-isotope-ratio

574   and gas-ratio measurement results. Rapid Commun. Mass Spectrom. 25, 2538–2560.

575   https://doi.org/10.1002/rcm.5129

576   Dawson, R.N., Murphy, K.L., 1972. The temperature dependency of biological denitrification.

577   Water Res. 6, 71–83. https://doi.org/10.1016/0043-1354(72)90174-1

578   Dogramaci, S.., Herczeg, A.., Schiff, S.., Bone, Y., 2001. Controls on $\delta^{34}S$ and $\delta^{18}O$ of dissolved

579   sulfate in aquifers of the Murray Basin, Australia and their use as indicators of flow

580   processes. Appl. Geochemistry 16, 475–488. https://doi.org/10.1016/S0883-
581   2927(00)00052-4

582 Estrada, N.L., Böhlke, J.K., Sturchio, N.C., Gu, B., Harvey, G., Burkey, K.O., Grantz, D.A.,
583   McGrath, M.T., Anderson, T.A., Rao, B., Sevanthi, R., Hatzinger, P.B., Jackson, W.A.,
584   2017. Stable isotopic composition of perchlorate and nitrate accumulated in plants:
585   Hydroponic experiments and field data. Sci. Total Environ. 595, 556–566.
586   https://doi.org/10.1016/j.scitotenv.2017.03.223

587 Fukada, T., Hiscock, K.M., Dennis, P.F., Grischek, T., 2003. A dual isotope approach to identify
588   denitrification in groundwater at a river-bank infiltration site. Water Res. 37, 3070–3078.
589   https://doi.org/10.1016/S0043-1354(03)00176-3

590 Ge, S., Peng, Y., Wang, S., Lu, C., Cao, X., Zhu, Y., 2012. Nitrite accumulation under constant
591   temperature in anoxic denitrification process: The effects of carbon sources and
592   COD/NO3-N. Bioresour. Technol. 114, 137–143.
593   https://doi.org/10.1016/j.biortech.2012.03.016

594 Giles, M., Morley, N., Baggs, E.M., Daniell, T.J., 2012. Soil nitrate reducing processes - Drivers,
595   mechanisms for spatial variation, and significance for nitrous oxide production. Front.
596   Microbiol. 3, 1–16. https://doi.org/10.3389/fmicb.2012.00407

597 Grau-Martínez, A., Torrentó, C., Carrey, R., Rodríguez-Escales, P., Domènech, C., Ghiglieri, G.,
598   Soler, A., Otero, N., 2017. Feasibility of two low-cost organic substrates for inducing
599   denitrification in artificial recharge ponds: Batch and flow-through experiments. J. Contam.
600   Hydrol. 198, 48–58. https://doi.org/10.1016/j.jconhyd.2017.01.001

601 Gumbricht, T., 1993. Nutrient removal capacity in submersed macrophyte pond systems in a
602   temperature climate. Ecol. Eng. 2, 49–61. https://doi.org/10.1016/0925-8574(93)90026-C

603 Ilyas, H., Masih, I., 2017. The performance of the intensified constructed wetlands for organic
604   matter and nitrogen removal: A review. J. Environ. Manage. 198, 372–383.
605   https://doi.org/10.1016/j.jenvman.2017.04.098

606 Jacobs, A.E., Harrison, J.A., 2014. Effects of floating vegetation on denitrification, nitrogen

607   retention, and greenhouse gas production in wetland microcosms. Biogeochemistry 119,

608   51–66. https://doi.org/10.1007/s10533-013-9947-9

609   Kang, Y., Zhang, J., Li, B., Zhang, Y., Sun, H., Hao Ngo, H., Guo, W., Xie, H., Hu, Z., Zhao, C.,

610   2018. Improvement of bioavailable carbon source and microbial structure toward

611   enhanced nitrate removal by Tubifex tubifex. Chem. Eng. J. 353, 699–707.

612   https://doi.org/10.1016/j.cej.2018.07.182

613   Kelso, B.H.L., Smith, R. V., Laughlin, R.J., Lennox, S.D., 1997. Dissimilatory nitrate reduction in

614   anaerobic sediments leading to river nitrite accumulation. Appl. Environ. Microbiol. 63,

615   4679–4685.

616   Knowles, R., 1982. Denitrification. Microbiol. Rev. 46, 43–70.

617   Kong, L., Wang, Y. Bin, Zhao, L.N., Chen, Z.H., 2009. Enzyme and root activities in surface-flow

618   constructed wetlands. Chemosphere 76, 601–608.

619   https://doi.org/10.1016/j.chemosphere.2009.04.056

620   Kovacic, D.A., David, M.B., Gentry, L.E., Starks, K.M., Cooke, R.A., 2000. Effectiveness of

621   Constructed Wetlands in Reducing Nitrogen and Phosphorus Export from Agricultural Tile

622   Drainage. J. Environ. Qual. 29, 1262.

623   https://doi.org/10.2134/jeq2000.00472425002900040033x

624   Kraft, B., Tegetmeyer, H.E., Sharma, R., Klotz, M.G., Ferdelman, T.G., Hettich, R.L., Geelhoed,

625   J.S., Strous, M., 2014. The environmental controls that govern the end product of bacterial

626   nitrate respiration. Science (80). 345, 3–7.

627   Laverman, A.M., Pallud, C., Abell, J., Cappellen, P. Van, 2012. Comparative survey of potential

628   nitrate and sulfate reduction rates in aquatic sediments. Geochim. Cosmochim. Acta 77,

629   474–488. https://doi.org/10.1016/j.gca.2011.10.033

630   Lin, Y.F., Jing, S.R., Wang, T.W., Lee, D.Y., 2002. Effects of macrophytes and external carbon

631   sources on nitrate removal from groundwater in constructed wetlands. Environ. Pollut.

632   119, 413–420. https://doi.org/10.1016/S0269-7491(01)00299-8

633   Lu, S., Hu, H., Sun, Y., Yang, J., 2009. Effect of carbon source on the denitrification in

634   constructed wetlands. J. Environ. Sci. 21, 1036–1043. https://doi.org/10.1016/S1001-

635   0742(08)62379-7

636 Lund, L.., Horne, A.., Williams, A.., 1999. Estimating denitrification in a large constructed

637   wetland using stable nitrogen isotope ratios. Ecol. Eng. 14, 67–76.

638   https://doi.org/10.1016/S0925-8574(99)00020-8

639 Margalef-Marti, R., Carrey, R., Soler, A., Otero, N., 2019. Evaluating the potential use of a dairy

640   industry residue to induce denitrification in polluted water bodies: A flow-through

641   experiment. J. Environ. Manage. 245. https://doi.org/10.1016/j.jenvman.2019.03.086

642 Mariotti, A., Germon, J.C., Hubert, P., Kaiser, P., Letolle, R., Tardieux, A., Tardieux, P., 1981.

643   Experimental determination of nitrogen kinetic isotope fractionation: Some principles;

644   illustration for the denitrification and nitrification processes. Plant Soil 62, 413–430.

645   https://doi.org/10.1007/BF02374138

646 Mariotti, A., Landreau, A., Simon, B., 1988. [15]N isotope biogeochemistry and natural

647   denitrification process in groundwater: Application to the chalk aquifer of northern France.

648   Geochim. Cosmochim. Acta 52, 1869–1878. https://doi.org/10.1016/0016-7037(88)90010-

649   5

650 McIlvin, M.R., Altabet, M.A., 2005. Chemical conversion of nitrate and nitrite to nitrous oxide for

651   nitrogen and oxygen isotopic analysis in freshwater and seawater. Anal Chem 77, 5589–

652   5595. https://doi.org/10.1021/ac050528s

653 Merchán, D., Causapé, J., Abrahão, R., 2013. Impact of irrigation implementation on hydrology

654   and water quality in a small agricultural basin in Spain. Hydrol. Sci. J. 58, 1400–1413.

655   https://doi.org/10.1080/02626667.2013.829576

656 Merchán, D., Causapé, J., Abrahão, R., García-Garizábal, I., 2015. Assessment of a newly

657   implemented irrigated area (Lerma Basin, Spain) over a 10-year period. II: Salts and

658   nitrate exported. Agric. Water Manag. https://doi.org/10.1016/j.agwat.2015.04.019

659 Merchán, D., Otero, N., Soler, A., Causapé, J., 2014. Main sources and processes affecting

660   dissolved sulphates and nitrates in a small irrigated basin (Lerma Basin, Zaragoza, Spain):

661   Isotopic characterization. Agric. Ecosyst. Environ. 195, 127–138.

662   https://doi.org/10.1016/j.agee.2014.05.011

663   Peralta, A.L., Matthews, J.W., Flanagan, D.N., Kent, A.D., 2012. Environmental factors at

664   dissimilar spatial scales influence plant and microbial communities in restored wetlands.

665   Wetlands 32, 1125–1134. https://doi.org/10.1007/s13157-012-0343-3

666   Rivett, M.O., Buss, S.R., Morgan, P., Smith, J.W.N., Bemment, C.D., 2008. Nitrate attenuation

667   in groundwater: A review of biogeochemical controlling processes. Water Res. 42, 4215–

668   4232. https://doi.org/10.1016/j.watres.2008.07.020

669   Rogers, K.H., Breen, P.F., Chick, A.J., 1991. Nitrogen Removal in Experimental Wetland

670   Treatment Systems: Evidence for the Role of Aquatic Plants. Res. J. Water Pollut. Control

671   Fed. 63, 934–941.

672   Ryabenko, E., Altabet, M. a., Wallace, D.W.R., 2009. Effect of chloride on the chemical

673   conversion of nitrate to nitrous oxide for δ^{15}N analysis. Limnol. Oceanogr. Methods 7,

674   545–552. https://doi.org/10.4319/lom.2009.7.545

675   Scott, J.T., McCarthy, M.J., Gardner, W.S., Doyle, R.D., 2008. Denitrification, dissimilatory

676   nitrate reduction to ammonium, and nitrogen fixation along a nitrate concentration gradient

677   in a created freshwater wetland. Biogeochemistry 87, 99–111.

678   https://doi.org/10.1007/s10533-007-9171-6

679   Si, Z., Song, X., Wang, Y., Cao, X., Zhao, Y., Wang, B., Chen, Y., Arefe, A., 2018. Intensified

680   heterotrophic denitrification in constructed wetlands using four solid carbon sources:

681   Denitrification efficiency and bacterial community structure. Bioresour. Technol. 267, 416–

682   425. https://doi.org/10.1016/j.biortech.2018.07.029

683   Sirivedhin, T., Gray, K.A., 2006. Factors affecting denitrification rates in experimental wetlands:

684   Field and laboratory studies. Ecol. Eng. 26, 167–181.

685   https://doi.org/10.1016/j.ecoleng.2005.09.001

686   Soana, E., Balestrini, R., Vincenzi, F., Bartoli, M., Castaldelli, G., 2017. Mitigation of nitrogen

687   pollution in vegetated ditches fed by nitrate-rich spring waters. Agric. Ecosyst. Environ.

688   243, 74–82. https://doi.org/10.1016/j.agee.2017.04.004

689 Sobczak, W. V., Findlay, S., 2002. Variation in Bioavailability of Dissolved Organic Carbon

690   among Stream Hyporheic Flowpaths. Ecology 83, 3194–3209.

691 Søvik, A.K., Mørkved, P.T., 2008. Use of stable nitrogen isotope fractionation to estimate

692   denitrification in small constructed wetlands treating agricultural runoff. Sci. Total Environ.

693   392, 157–165. https://doi.org/10.1016/j.scitotenv.2007.11.014

694 Spieles, D.J., Mitsch, W.J., 1999. The effects of season and hydrologic and chemical loading on

695   nitrate retention in constructed wetlands: A comparison of low- and high-nutrient riverine

696   systems. Ecol. Eng. 14, 77–91. https://doi.org/10.1016/S0925-8574(99)00021-X

697 Spoelstra, J., Schiff, S.L., Semkin, R.G., Jeffries, D.S., Elgood, R.J., 2010. Nitrate attenuation in

698   a small temperate wetland following forest harvest. For. Ecol. Manage. 259, 2333–2341.

699   https://doi.org/10.1016/j.foreco.2010.03.006

700 Strebel, O., Böttcher, J., Fritz, P., 1990. Use of isotope fractionation of sulfate-sulfur and sulfate-

701   oxygen to assess bacterial desulfurication in a sandy aquifer. J. Hydrol. 121, 155–172.

702   https://doi.org/10.1016/0022-1694(90)90230-U

703 Tanner, C.C., Nguyen, M.L., Sukias, J.P.S., 2005. Nutrient removal by a constructed wetland

704   treating subsurface drainage from grazed dairy pasture. Agric. Ecosyst. Environ. 105,

705   145–162. https://doi.org/10.1016/j.agee.2004.05.008

706 Trois, C., Coulon, F., de Combret, C.P., Martins, J.M.F., Oxarango, L., 2010. Effect of pine bark

707   and compost on the biological denitrification process of non-hazardous landfill leachate:

708   Focus on the microbiology. J. Hazard. Mater. 181, 1163–1169.

709   https://doi.org/10.1016/j.jhazmat.2010.05.077

710 Uusheimo, S., Tulonen, T., Aalto, S.L., Arvola, L., 2018. Mitigating agricultural nitrogen load with

711   constructed ponds in northern latitudes: A field study on sedimental denitrification rates.

712   Agric. Ecosyst. Environ. 261, 71–79. https://doi.org/10.1016/j.agee.2018.04.002

713 Vidal-Gavilan, G., Folch, A., Otero, N., Solanas, A.M., Soler, A., 2013. Isotope characterization

714   of an in situ biodenitrification pilot-test in a fractured aquifer. Appl. Geochemistry 32, 153–

715   163. https://doi.org/10.1016/j.apgeochem.2012.10.033

716   Vitousek, P.M., Aber, J.D., Howarth, R.W., Likens, G.E., Matson, P.A., Schindler, D.W.,

717   Schlesinger, W.H., Tilman, D.G., 1997. Summary for Policymakers, in: Intergovernmental

718   Panel on Climate Change (Ed.), Climate Change 2013 - The Physical Science Basis.

719   Cambridge University Press, Cambridge, pp. 1–30.

720   https://doi.org/10.1017/CBO9781107415324.004

721   Vymazal, J., 2007. Removal of nutrients in various types of constructed wetlands. Sci. Total

722   Environ. 380, 48–65. https://doi.org/10.1016/j.scitotenv.2006.09.014

723   Ward, M.H., DeKok, T.M., Levallois, P., Brender, J., Gulis, G., Nolan, B.T., VanDerslice, J.,

724   2005. Workgroup Report: Drinking-Water Nitrate and Health—Recent Findings and

725   Research Needs. Environ. Health Perspect. 113, 1607–1614.

726   https://doi.org/10.1289/ehp.8043

727   Warneke, S., Schipper, L.A., Matiasek, M.G., Scow, K.M., Cameron, S., Bruesewitz, D.A.,

728   McDonald, I.R., 2011. Nitrate removal, communities of denitrifiers and adverse effects in

729   different carbon substrates for use in denitrification beds. Water Res. 45, 5463–5475.

730   https://doi.org/10.1016/j.watres.2011.08.007

731   Wu, H., Zhang, J., Ngo, H.H., Guo, W., Hu, Z., Liang, S., Fan, J., Liu, H., 2015. A review on the

732   sustainability of constructed wetlands for wastewater treatment: Design and operation.

733   Bioresour. Technol. 175, 594–601. https://doi.org/10.1016/j.biortech.2014.10.068

734

Figure 1. CW design. Photograph of the surface flow CW with emergent macrophytes. The sampling points are depicted by white squares (H1 to H6), and the water flow within the CW with striped arrows. Non-treated water flow discharging to the Lerma gully is depicted with black arrows, and that of treated water with a white arrow.

Figure 2. Evolution of denitrification in the biostimulated microcosms. NO_3^- (circles joined by a continuous line) and NO_2^- (squares joined by a dashed line) measured in (**A**) the batch experiments employing different C sources and (**B**) the experiments testing the effects of temperature and lifespan of the stubble.

Figure 3. NO_3^--O and NO_3^--N isotopic fractionation throughout denitrification in the biostimulated microcosms. Results from the batch experiments testing (**A, B**) different C sources and (**C, D**) the effects of temperature and lifespan of the stubble.

Figure 4. NO_3^- attenuation in the CW before the application of stubble. Black circles depict the sampling campaigns performed at a ~5.5 L/s flow rate (full symbols for the campaign of June 14, 2017 and empty symbols for that of September 5, 2017), and grey circles depict the sampling campaigns performed at a ~2.5 L/s flow rate (September 12, 2017). (**A**) NO_3^- concentration along the CW flow direction, where dashed lines represent the range of NO_3^- concentrations measured at the inlet of the CW throughout the study period. (**B**) Isotopic characterization including the regression line, where the dashed square represents the range of isotopic compositions measured at the inlet of the CW throughout the study period.

Figure 5. NO_3^- attenuation in the CW after the first application of stubble in autumn. (**A**) NO_3^- concentration along the CW, where dashed lines represent the range of NO_3^- concentrations measured at the inlet of the CW throughout the study period. Full symbols depict the sampling campaign conducted on October 2, 2017, and empty symbols depict that conducted on October 10, 2017 (seven and fourteen days after the application of the stubble, respectively). (**B, C**) NO_3^- concentrations monitored at the inlet (black) and outlet (grey) in the days before and after the sampling campaigns, respectively.

Figure 6. NO$_3^-$ attenuation in the CW after the second application of stubble in spring. (**A**) NO$_3^-$ concentrations monitored at the inlet (black) and outlet (grey) of the CW throughout the first days of treatment. (**B)** NO$_3^-$ concentrations along the CW flow direction, for each sampling campaign. Dashed lines represent the range of NO$_3^-$ concentrations measured at the inlet of the CW throughout the study period. The 7 sampling campaigns performed throughout the 100 days after stubble application are represented by shades of grey (from darker to lighter as time progressed), with the last represented by the empty symbols. The campaign performed before application is represented by asterisks.

Figure 7. Denitrification efficiency in the CW determined from the laboratory-obtained ε values. Isotopic values obtained from the samples collected at the CW, including the regression line (black). The three denitrification % lines (grey) presented correspond to the three conditions tested in the laboratory that were closest to the CW conditions throughout the field-scale test.

Figure 8. Dissolved organic C in the CW before and after application of stubble. NPDOC concentration along the CW flow. The 5 sampling campaigns conducted within the 63 days after stubble application are presented in shades of grey, from darkest to lightest as time progressed. The campaign performed before application is represented by asterisks.

A

Stubble 24 ºC ●
Compost 24 ºC ●
Hay 24 ºC ●

B

Decomposed stubble 24 ºC ○
Stubble 24 ºC ●
Stubble 16 ºC ●
Stubble 8 ºC ●

A

Stubble 24 ºC
y = -0.0283x + 0.0035
R² = 0.99

Hay 24 ºC
y = -0.018x + 0.0024
R² = 0.68

Compost 24 ºC
y = -0.0126x + 0.0033
R² = 0.95

$Ln(Rr/Ri)$ $\delta^{18}O$-NO_3^-

$Ln(Cr/Ci)$ NO_3^-

B

Stubble 24 ºC
y = -0.0233x + 0.0033
R² = 0.97

Hay 24 ºC
y = -0.0319x + 0.0031
R² = 0.91

Compost 24 ºC
y = -0.0105x + 0.0005
R² = 0.96

$Ln(Rr/Ri)$ $\delta^{15}N$-NO_3^-

$Ln(Cr/Ci)$ NO_3^-

C

Stubble 24 ºC
y = -0.0283x + 0.0035
R² = 0.99

Stubble 16 ºC
y = -0.0304x + 0.0024
R² = 0.98

Stubble 8 ºC
y = -0.0097x + 0.002
R² = 0.62

Decomposed
stubble 24 ºC
y = -0.0212x - 0.0026
R² = 0.95

$Ln(Rr/Ri)$ $\delta^{18}O$-NO_3^-

$Ln(Cr/Ci)$ NO_3^-

D

Stubble 24ºC
y = -0.0233x + 0.0033
R² = 0.97

Stubble 16ºC
y = -0.0283x + 0.0059
R² = 0.96

Stubble 8ºC
y = -0.0157x + 0.0027
R² = 0.66

Decomposed
stubble 24 ºC
y = -0.0225x - 0.0031
R² = 0.97

$Ln(Rr/Ri)$ $\delta^{15}N$-NO_3^-

$Ln(Cr/Ci)$ NO_3^-

A

NO₃⁻ (mM) vs CW sampling point

High flow

Low flow

B

δ¹⁸O-NO₃⁻ (‰) vs δ¹⁵N-NO₃⁻ (‰)

y = 0.84x − 0.07
R² = 0.91

0.8 mM

1.6 mM

A

NO$_3^-$ (mM) vs CW sampling point

- ● 7 (02/10/2017)
- ○ 14 (10/10/2017)

B

NO$_3^-$ (mM) vs Day

Inlet

Outlet

C

NO$_3^-$ (mM) vs Day

Inlet

Outlet

A

B

- 0 (11/05/2018)
- 7 (18/05/2018)
- 14 (25/05/2018)
- 32 (12/06/2018)
- 63 (13/07/2018)
- 100 (19/08/2018)
- 125 (13/09/2018)
- 161 (19/10/2018)

Legend:
- 0 (11/05/2018)
- 7 (18/05/2018)
- 14 (25/05/2018)
- 32 (12/06/2018)
- 63 (13/07/2018)
- 100 (19/08/2018)
- 125 (13/09/2018)
- 161 (19/10/2018)

Y-axis: NPDOC (mM)

X-axis: CW sampling point

Table 1. Series of experiments. Tested conditions and composition of microcosms. DIW = deionized water.

Series	Condition	Code	C source	Material (g)	C (g/L)	Water source (100 mL)	Temperature (ºC)
I	Biostimulated	C-24	Animal compost	0.25	0.8	Wetland	24
	Control	C-24-blank	Animal compost	0.25	0.8	DIW	24
II	Biostimulated	H-24	Wheat hay	1	4.2	Wetland	24
	Control	H-24-blank	Wheat hay	1	4.2	DIW	24
III	Biostimulated	S-24	Corn stubble	1	3.6	Wetland	24
	Control	S-24-blank	Corn stubble	1	3.6	DIW	24
IV	Biostimulated	S-16	Corn stubble	1	3.6	Wetland	16
	Control	S-16-blank	Corn stubble	1	3.6	DIW	16
V	Biostimulated	S-8	Corn stubble	1	3.6	Wetland	8
	Control	S-8-blank	Corn stubble	1	3.6	DIW	8
VI	Biostimulated	DS-24	Decomposed stubble	1	3.6	Wetland	24
	Control	DS-24-blank	Decomposed stubble	1	3.6	DIW	24

Table 2. Sampling campaigns. Sampling dates and operation mode of the CW for all sampling campaigns (six samples each).

Test period	Date	Days since stubble addition	Operation mode	Observations
I	14/06/2017	-	High flow	No external organic C addition
	05/09/2017	-	High flow	
	12/09/2017	-	Low flow	
II	02/10/2017	7	High flow	First organic C source addition on 25/09/2017
	10/10/2017	14		
III	11/05/2018	0	High flow	Second organic C source addition on 11/05/2018
	18/05/2018	7		
	25/05/2018	14		
	12/06/2018	32		
	13/07/2018	63		
	19/08/2018	100		
	13/09/2018	125		
	19/10/2018	161		

Table 3. Waste products composition. C and N concentrations and isotopic composition of the corn stubble, wheat hay, and animal compost employed to promote denitrification.

SOURCE	C (%)	N (%)	δ^{13}C (‰)	δ^{15}N (‰)
Animal compost	32.1	3.1	-25.4	10.8
Wheat hay	40.9	0.4	-27.8	3.0
Corn stubble	36.1	1.0	-13.6	6.7

Table 4. Calculated ε values from the laboratory microcosms. $\varepsilon^{18}O_{NO3/N2}$, $\varepsilon^{15}N_{NO3/N2}$, and $\varepsilon^{15}N_{NO3/N2}/\varepsilon^{18}O_{NO3/N2}$ for each condition tested at laboratory-scale.

EXPERIMENT	$\varepsilon^{18}O_{NO3/N2}$	$\varepsilon^{15}N_{NO3/N2}$	$\varepsilon^{15}N/\varepsilon^{18}O$
Compost 24⁰C	-12.6	-10.5	0.8
Hay 24⁰C	-18.0	-31.9	1.8
Stubble 24⁰C	-28.3	-23.3	0.8
Stubble 16⁰C	-30.4	-28.3	0.9
Stubble 8⁰C	-9.7	-15.7	1.6
Decomposed stubble 24⁰C	-21.2	-22.5	1.1

Supporting Information, section S1: δ^{13}C-DIC results

The δ^{13}C-DIC results provided information about the transformation of organic C from the waste materials to inorganic C (**Equation S1**). These results are presented in Supporting Information **Table S2**. As DIC concentration increased, the initial δ^{13}C-DIC in water of -13.1 ‰ decreased to -15.5 ‰ and -20.0 ‰ in the microcosms containing hay and compost, respectively, but remained unchanged in the stubble experiment (**Figure S2**). The flat trend observed in the experiments with stubble, in contrast to the correlations obtained with the experiments employing hay and compost, was attributed to the intrinsic δ^{13}C-C_{bulk} of each material (**Table 3**). The most significant change in the δ^{13}C-DIC was observed for the experiment involving hay, which presented a lower δ^{13}C-C_{bulk} (-27.8 ‰) compared to that of compost (-25.4‰); stubble did not produce any change because its δ^{13}C-C_{bulk} (-13.6 ‰) is close to the δ^{13}C-DIC of water (-13.1 ‰). Hay and stubble presented a different intrinsic δ^{13}C-C_{bulk} as they are classified as C4 and C3 plants, respectively (Leary, 1988). An isotopic fractionation effect derived from the bacterial C metabolism did not seem to be significant under the tested conditions. These results show that the δ^{13}C-DIC analysis can be applied to assess the efficiency of biostimulation strategies at field-scale when C sources with an intrinsic δ^{13}C-C_{bulk} differing from the δ^{13}C-DIC of water (such as C4 plant materials) are used.
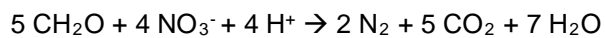
$$5\ CH_2O + 4\ NO_3^- + 4\ H^+ \rightarrow 2\ N_2 + 5\ CO_2 + 7\ H_2O \qquad \textbf{Equation S1}$$

References:

Leary, M.H.O., 1988. Carbon Isotopes in Photosynthesis. Bioscience 38, 328–336.

A

NO$_3^-$ (mM) axis: 0, 20, 40, 60, 80, 100, 120

Inlet

Outlet

X-axis (Day): 08/05/2018, 10/05/2018, 12/05/2018, 14/05/2018, 16/05/2018, 18/05/2018, 20/05/2018, 22/05/2018, 24/05/2018, 26/05/2018, 28/05/2018, 30/05/2018, 01/06/2018, 03/06/2018, 05/06/2018, 07/06/2018, 09/06/2018, 11/06/2018, 13/06/2018, 15/06/2018

B

NO$_3^-$ (mM) axis: 0, 20, 40, 60, 80, 100, 120

Inlet

Outlet

X-axis (Day): 01/07/2018, 03/07/2018, 05/07/2018, 07/07/2018, 09/07/2018, 11/07/2018, 13/07/2018, 15/07/2018, 17/07/2018, 19/07/2018, 21/07/2018, 23/07/2018, 25/07/2018, 27/07/2018, 29/07/2018, 31/07/2018, 02/08/2018, 04/08/2018, 06/08/2018, 08/08/2018, 10/08/2018, 12/08/2018, 14/08/2018, 16/08/2018, 18/08/2018, 20/08/2018, 22/08/2018, 24/08/2018, 26/08/2018, 28/08/2018, 30/08/2018, 01/09/2018

Figure S1. Monitored NO$_3^-$ concentrations at the inlet and outlet of the CW during the third period of the test. The NO$_3^-$ retention time in the CW was considered for the outlet data. (**A**) May-June 2018, (**B**) July-August 2018 and (**C**) September-October 2018. The data between 10/05/2018 and 06/06/2018 and between 13/06/2018 and 01/07/2018 is lacking due to technical issues.
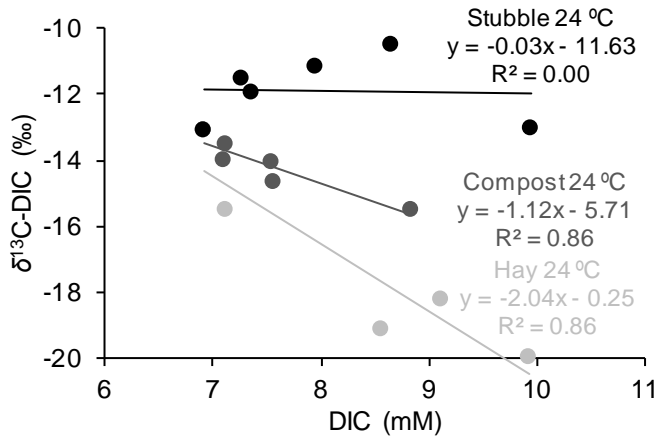
Figure S2. Relationship between δ^{13}C-DIC and DIC concentration throughout denitrification.

Correlation between δ^{13}C-DIC and DIC concentration in the samples collected from laboratory batch experiments testing different C sources for the induction of the bacterial NO_3^- reduction.

Table S1. Precipitation and temperature records. Data collected from a meteorological station near the CW (coordinates X = 649168.18 and Y = 4662201.55).

Month	Precipitation (mm)	Average temperature (ºC)	Minimum temperature (ºC)	Maximum temperature (ºC)
June-17	80.2	23.2	13.2	30.2
July-17	46.6	23.6	15.1	28.3
August-17	79.4	23.2	16.5	29.1
September-17	47.2	17.6	12.5	23.3
October-17	11.1	16.0	10.3	20.4
November-17	13.1	8.6	2.5	15.3
December-17	17.3	5.1	0.3	9.4
January-18	64.5	6.8	2.0	12.7
February-18	37.6	4.9	0.9	10.0
March-18	82.8	8.5	3.8	12.3
April-18	173.9	12.8	5.8	16.8
May-18	54.7	15.8	9.6	20.0
June-18	17.3	20.9	15.8	26.2
July-18	44.2	24.6	19.9	28.4
August-18	4.4	23.8	19.1	28.2
September-18	19.7	21.2	15.9	23.9
October-18	0.0	16.3	13.1	18.8

Table S2. Standards for isotopic analysis. International and laboratory (CCiT) standards used

for normalization of the results.

Analysis	Standards
$\delta^{15}N\text{-}NO_3^-$	USGS-32, USGS-34, USGS-35 and CCiT-IWS ($\delta^{15}N$ = +16.9 ‰)
$\delta^{18}O\text{-}NO_3^-$	USGS-32, USGS-34, USGS-35 and CCiT-IWS ($\delta^{18}O$ = +28.5 ‰)
$\delta^{15}N\text{-}N_{bulk}$	USGS-40, IAEA-N1, IAEA-NO3, IAEA-N2
$\delta^{13}C\text{-}C_{bulk}$	USGS-40, IAEA-CH7, IAEA-CH6
$\delta^{13}C\text{-}DIC$	CCiT-NaHCO$_3$ ($\delta^{13}C$ = -4.4 ‰), CCiT-NaKHCO$_3$ ($\delta^{13}C$ = -18.7 ‰) and CCiT-KHCO$_3$ ($\delta^{13}C$ = +29.2 ‰)
$\delta^{34}S\text{-}SO_4^{2-}$	NBS-127, SO5, SO6 and CCiT-YCEM ($\delta^{34}S$ = +12.8 ‰)
$\delta^{18}O\text{-}SO_4^{2-}$	NBS-127, SO6, USGS-34, CCiT-YCEM ($\delta^{18}O$ = +17.6 ‰) and CCiT-ACID ($\delta^{18}O$ = +13.2 ‰)

Table S3. Batch experiments results. N and C compounds concentration and isotopic composition.

Code	Hour	NO_3^- (mM)	NO_2^- (mM)	NH_4^+ (mM)	N_2O (nmol)	N_2O (%)*	NPDOC (mM)	DIC (mM)	$\delta^{15}N$-NO_3^- (‰)	$\delta^{18}O$-NO_3^- (‰)	$\delta^{13}C$-DIC (‰)
CW water	0.0	2.1	0.0	0.0	n.d.	n.d.	0.5	6.9	6.4	4.9	-13.1
C-24-1	14.0	2.0	0.0	0.1	n.d.	n.d.	10.2	7.1	4.6	5.7	-13.5
C-24-2	14.5	1.9	0.1	0.1	n.d.	n.d.	n.d.	n.d.	6.7	8.5	n.d.
C-24-3	20.0	1.8	0.3	0.1	n.d.	n.d.	9.0	7.1	9.3	10.6	-14.0
C-24-4	21.5	1.6	0.3	0.1	n.d.	n.d.	n.d.	n.d.	11.6	13.8	n.d.
C-24-5	24.5	1.5	0.4	0.1	n.d.	n.d.	10.6	7.5	13.1	15.2	-14.1
C-24-6	38.0	0.9	0.7	0.1	n.d.	n.d.	8.8	7.6	17.0	22.6	-14.7
C-24-7	62.0	0.5	0.3	0.1	n.d.	n.d.	n.d.	n.d.	21.2	28.9	n.d.
C-24-8	89.0	0.3	0.1	n.d.	n.d.	n.d.	5.3	8.8	24.5	30.0	-15.5
C-24-9	94.0	0.2	0.1	n.d.	n.d.	n.d.	n.d.	n.d.	36.4	41.0	n.d.
C-24-10	96.0	0.0	0.0	n.d.	n.d.	n.d.	7.8	n.d.	n.d.	n.d.	n.d.
C-24-blank	188.0	0.0	0.0	n.d.	n.d.	n.d.	14.3	n.d.	n.d.	n.d.	n.d.
H-24-1	13.8	2.1	0.1	0.1	n.d.	n.d.	14.7	n.d.	10.3	9.5	-18.3
H-24-2	15.0	1.8	0.3	0.1	n.d.	n.d.	13.4	9.1	15.2	12.7	-18.3
H-24-3	15.5	1.7	0.6	n.d.	n.d.	n.d.	n.d.	n.d.	12.3	5.8	n.d.
H-24-4	15.8	1.9	0.5	n.d.	n.d.	n.d.	n.d.	n.d.	12.4	6.3	n.d.
H-24-5	17.8	1.2	0.8	0.0	n.d.	n.d.	11.8	n.d.	34.5	25.1	-17.7
H-24-6	18.0	1.5	1.0	n.d.	n.d.	n.d.	n.d.	n.d.	23.3	15.9	n.d.
H-24-7	20.0	0.8	1.5	n.d.	n.d.	n.d.	n.d.	n.d.	37.0	20.7	n.d.
H-24-8	22.5	0.0	1.2	0.0	n.d.	n.d.	12.5	8.6	n.d.	n.d.	-19.2
H-24-9	38.5	0.0	0.0	0.2	n.d.	n.d.	14.7	9.9	n.d.	n.d.	-20.0
H-24-blank-1	4.0	0.1	0.0	0.0	n.d.	n.d.	n.d.	n.d.	n.d.	n.d.	n.d.
H-24-blank-2	38.5	0.0	0.0	n.d.	n.d.	n.d.	16.9	1.8	n.d.	n.d.	n.d.
S-24-1	13.0	2.2	0.0	0.2	n.d.	n.d.	14.7	9.9	7.8	8.0	-13.0
S-24-2	13.3	2.1	0.1	n.d.	n.d.	n.d.	n.d.	n.d.	n.d.	n.d.	-11.4
S-24-3	14.0	1.8	0.3	n.d.	n.d.	n.d.	15.7	7.3	11.9	10.3	-11.6
S-24-4	14.8	1.7	0.3	n.d.	n.d.	n.d.	n.d.	n.d.	n.d.	n.d.	n.d.
S-24-5	15.5	1.8	0.3	0.3	n.d.	n.d.	18.2	7.4	17.2	17.5	-12.0
S-24-6	17.5	0.3	1.3	n.d.	n.d.	n.d.	13.2	n.d.	59.4	60.8	n.d.
S-24-7	18.5	0.3	1.3	0.1	n.d.	n.d.	n.d.	n.d.	61.1	73.8	n.d.
S-24-8	19.5	0.2	1.4	n.d.	n.d.	n.d.	n.d.	n.d.	62.0	76.1	n.d.
S-24-9	21.0	0.0	1.4	0.1	n.d.	n.d.	n.d.	n.d.	n.d.	n.d.	n.d.
S-24-10	22.3	0.0	1.5	n.d.	n.d.	n.d.	15.9	8.0	n.d.	n.d.	-11.2
S-24-11	23.8	0.0	1.1	n.d.	n.d.	n.d.	n.d.	n.d.	n.d.	n.d.	n.d.
S-24-12	38.5	0.0	0.0	1.0	n.d.	n.d.	18.5	8.7	n.d.	n.d.	-10.5
S-24-blank-1	38.5	0.1	0.0	0.0	n.d.	n.d.	27.3	n.d.	n.d.	n.d.	n.d.
CW water	0.0	1.9	0.0	n.d.	n.d.	n.d.	n.d.	n.d.	5.9	8.0	n.d.
S-16-1	25.0	1.8	0.2	n.d.	0.8	0.001	n.d.	n.d.	17.4	14.3	n.d.
S-16-2	27.0	1.3	0.1	n.d.	0.6	0.001	n.d.	n.d.	20.5	20.5	n.d.

S-16-3	30.0	1.0	0.5	n.d.	n.d.	n.d.	n.d.	n.d.	28.7	29.8	n.d.
S-16-4	32.0	0.6	0.8	n.d.	2.5	0.002	n.d.	n.d.	46.2	39.7	n.d.
S-16-5	34.0	0.3	1.2	n.d.	n.d.	n.d.	n.d.	n.d.	62.1	68.6	n.d.
S-16-6	39.0	0.0	1.7	n.d.	8.7	0.009	n.d.	n.d.	n.d.	n.d.	n.d.
S-16-7	42.0	0.0	1.8	n.d.	1.9	0.002	n.d.	n.d.	n.d.	n.d.	n.d.
S-16-8	46.0	0.0	0.7	n.d.	0.4	0.000	n.d.	n.d.	n.d.	n.d.	n.d.
S-16-9	50.0	0.0	0.8	n.d.	1.1	0.001	n.d.	n.d.	n.d.	n.d.	n.d.
S-16-10	64.0	0.0	0.0	n.d.	n.d.	n.d.	n.d.	n.d.	n.d.	n.d.	n.d.
S-8'-1	66.0	1.6	0.0	n.d.	n.d.	n.d.	n.d.	n.d.	9.0	10.1	n.d.
S-8'-2	99.0	1.3	0.3	n.d.	n.d.	n.d.	n.d.	n.d.	13.6	13.0	n.d.
S-8'-3	114.0	0.9	0.3	n.d.	n.d.	n.d.	n.d.	n.d.	16.4	15.7	n.d.
S-8-1	66.0	1.7	0.1	n.d.	1.5	0.001	n.d.	n.d.	15.0	17.4	n.d.
S-8-2	75.0	1.2	0.2	n.d.	1.8	0.002	n.d.	n.d.	22.9	n.d.	n.d.
S-8-3	90.0	0.7	0.6	n.d.	2.0	0.002	n.d.	n.d.	24.3	20.6	n.d.
S-8-4	99.0	0.0	1.2	n.d.	5.1	0.005	n.d.	n.d.	n.d.	n.d.	n.d.
S-8-5	114.0	0.0	0.9	n.d.	2.8	0.003	n.d.	n.d.	n.d.	n.d.	n.d.
S-8-6	123.0	0.0	0.7	n.d.	0.0	0.000	n.d.	n.d.	n.d.	n.d.	n.d.
S-8-7	138.0	0.0	0.7	n.d.	3.4	0.003	n.d.	n.d.	n.d.	n.d.	n.d.
S-8-8	147.0	0.0	0.0	n.d.	0.6	0.001	n.d.	n.d.	n.d.	n.d.	n.d.
CW water	0.0	1.4	0.0	n.d.	n.d.	n.d.	0.5	n.d.	14.5	13.4	n.d.
DS-24-1	3.5	1.4	0.0	n.d.	n.d.	n.d.	n.d.	n.d.	n.d.	n.d.	n.d.
DS-24-2	5.5	1.3	0.1	0.1	n.d.	n.d.	2.2	n.d.	13.5	12.8	n.d.
DS-24-3	6.0	0.6	0.1	0.0	2.9	0.003	1.7	n.d.	25.2	23.9	n.d.
DS-24-4	7.5	0.8	0.3	n.d.	n.d.	n.d.	n.d.	n.d.	21.5	19.3	n.d.
DS-24-5	9.0	0.2	0.5	n.d.	1.6	0.002	1.9	n.d.	53.1	55.0	n.d.
DS-24-6	9.5	0.0	0.7	1.3	n.d.	n.d.	2.5	n.d.	n.d.	n.d.	n.d.
DS-24-7	10.5	0.6	0.4	n.d.	n.d.	n.d.	n.d.	n.d.	n.d.	n.d.	n.d.
DS-24-8	11.0	0.9	0.8	n.d.	5.4	0.005	n.d.	n.d.	26.7	28.6	n.d.
DS-24-9	12.5	0.0	0.3	n.d.	n.d.	n.d.	n.d.	n.d.	n.d.	n.d.	n.d.
DS-24-10	13.3	0.6	0.5	1.0	n.d.	n.d.	n.d.	n.d.	28.1	27.6	n.d.
DS-24-11	14.0	0.0	0.5	n.d.	n.d.	n.d.	1.7	n.d.	n.d.	n.d.	n.d.
DS-24-12	15.0	0.0	0.5	n.d.	n.d.	n.d.	n.d.	n.d.	n.d.	n.d.	n.d.
DS-24-13	17.0	0.6	0.5	n.d.	15.1	0.015	n.d.	n.d.	33.3	24.2	n.d.
DS-24-14	17.0	0.4	0.6	0.9	11.7	0.012	n.d.	n.d.	44.3	43.6	n.d.
DS-24-15	20.0	0.0	0.4	0.3	n.d.	n.d.	n.d.	n.d.	n.d.	n.d.	n.d.
DS-24-16	20.3	0.1	0.5	n.d.	12.7	0.013	n.d.	n.d.	78.5	70.7	n.d.
DS-24-17	22.0	0.0	0.6	n.d.	n.d.	n.d.	n.d.	n.d.	n.d.	n.d.	n.d.
DS-24-18	23.0	0.0	0.0	0.5	n.d.	n.d.	8.8	n.d.	n.d.	n.d.	n.d.
DS-24-19	24.0	0.0	0.2	n.d.	n.d.	n.d.	1.7	n.d.	n.d.	n.d.	n.d.

* % of initial NO_3^-–N found as N_2O-N

n.d. = non determined

NH_4^+ in the DS-24 experiment was analyzed by ion selective electrode while in the others by spectrophotometry

Table S4. ICP data. Major cations and trace elements concentration measured in the samples from the laboratory experiments (semiquantitative).

Code	Hour	Na	S	Ca	Mg	K	Si	Sr	P	B	Li	Mn	Zn	Cu	Fe	Ba	V	Co	Tl	Cd	Cr
CW water	0.0	326.8	146.3	130.7	99.3	6.2	10.9	4.2	-	0.35	0.12	-	-	0.08	0.01	0.06	0.06	0.01	0.14	-	0.01
C-24-1	14.0	345.0	163.0	125.8	103.4	65.4	11.4	3.9	1.4	0.42	0.13	0.05	0.09	0.04	0.10	0.05	0.07	-	-	-	-
C-24-2	14.5	334.6	151.1	125.4	101.2	43.3	11.1	3.9	0.8	0.39	0.13	0.05	0.06	0.04	0.07	0.05	0.07	0.01	-	-	-
C-24-3	20.0	321.8	151.8	124.0	100.4	58.2	10.9	3.8	1.0	0.40	0.12	0.06	0.07	0.03	0.08	0.05	0.07	-	0.15	-	-
C-24-5	24.5	328.7	160.1	123.2	102.8	68.7	11.3	3.8	1.2	0.42	0.13	0.08	0.11	0.04	0.11	0.05	0.07	-	-	-	-
C-24-6	38.0	325.2	152.3	123.1	104.6	51.6	11.4	3.6	1.4	0.41	0.13	0.11	0.11	0.04	0.12	0.04	0.07	-	-	-	-
C-24-8	89.0	334.2	151.7	125.6	104.5	41.5	12.1	3.6	1.4	0.40	0.13	0.12	0.05	0.05	0.07	0.04	0.07	-	-	0.01	-
H-24-1	13.8	360.3	168.3	139.4	102.3	160.1	22.8	4.3	0.6	0.38	0.13	0.04	0.04	0.03	0.02	0.11	0.07	0.02	-	0.01	-
H-24-2	15.0	362.0	165.3	139.5	105.0	130.8	22.2	4.2	2.3	0.38	0.13	0.05	0.04	0.03	0.02	0.24	0.06	-	-	-	-
H-24-5	17.8	371.4	170.9	141.4	103.0	142.1	22.1	4.3	-	0.38	0.13	0.06	0.05	0.03	0.01	0.11	0.06	-	-	-	-
H-24-8	22.5	365.1	169.0	140.9	103.4	180.9	25.1	4.3	-	0.37	0.13	0.06	0.06	0.03	0.02	0.16	0.07	0.01	-	-	-
H-24-9	38.5	355.7	164.3	140.4	104.1	167.2	31.2	4.4	0.8	0.37	0.13	0.04	0.06	0.03	0.01	0.13	0.06	-	-	-	-
S-24-1	13.0	318.9	155.5	136.2	108.1	130.8	13.4	4.0	1.2	0.48	0.12	0.10	0.09	0.07	0.06	0.08	0.07	-	-	-	-
S-24-2	13.3	324.5	146.8	128.6	101.5	75.5	13.6	3.8	1.6	0.36	0.12	0.11	0.05	0.05	0.04	0.07	0.06	0.01	-	-	-
S-24-3	14.0	325.3	148.8	126.4	101.4	118.2	13.0	3.7	2.2	0.38	0.12	0.13	0.03	0.04	0.04	0.07	0.06	-	0.15	-	-
S-24-5	15.5	329.9	151.8	130.2	103.2	78.9	14.4	3.8	1.4	0.39	0.12	0.17	0.03	0.04	0.04	0.08	0.06	-	-	-	-
S-24-10	22.3	318.4	149.4	130.9	104.5	108.7	13.9	3.8	0.8	0.39	0.13	0.12	0.04	0.05	0.04	0.12	0.07	-	-	-	-
S-24-12	38.5	329.2	150.0	139.0	109.9	99.5	14.4	4.0	1.1	0.39	0.13	0.16	0.04	0.06	0.05	0.10	0.07	0.03	-	-	0.01

All data is expressed as ppm. Hyphen = below detection limit. The Al, As, Be, Mo, Ni, Pb, Sb, Se and Ti were below detection limit in all analyzed samples.

Table S5. CW test results. Chemical and isotopic characterization of the samples collected in the CW previous and after the implementation of the bioremediation strategy.

Date	Point	NO_2^- (mM)	NO_3^- (mM)	NH_4^+ (mM)	DIC (mM)	NPDOC (mM)	SO_4^{2-} (mM)	$\delta^{13}C\text{-}DIC$ (‰)	$\delta^{15}N\text{-}NO_3^-$ (‰)	$\delta^{18}O\text{-}NO_3^-$ (‰)	$\delta^{34}S\text{-}SO_4^{2-}$ (‰)	$\delta^{18}O\text{-}SO_4^{2-}$ (‰)	NO_3^- attenuation %[1]	%[2]	kg/d
14/06/17	H1	0.0	1.4	n.d.	7.1	n.d.	n.d.	n.d.	6.4	7.2	0.8	12.5	n.d.	n.d.	n.d.
	H2	0.0	1.2	n.d.	6.9	n.d.	n.d.	n.d.	6.8	5.9	n.d.	n.d.	n.d.	n.d.	n.d.
	H3	0.0	1.4	n.d.	6.8	n.d.	n.d.	n.d.	6.8	6.5	1.8	12.7	n.d.	n.d.	n.d.
	H4	0.0	1.4	n.d.	n.d.	n.d.	n.d.	n.d.	8.1	6.7	n.d.	n.d.	n.d.	n.d.	n.d.
	H5	0.0	1.4	n.d.	6.9	n.d.	n.d.	n.d.	7.5	6.6	n.d.	n.d.	n.d.	n.d.	n.d.
	H6	0.0	1.2	n.d.	7.0	n.d.	n.d.	n.d.	8.3	6.1	2.5	12.4	n.d.	n.d.	n.d.
05/09/17	H1	0.0	1.3	0.0	7.5	0.6	n.d.	-12.9	11.6	8.7	n.d.	n.d.	n.d.	n.d.	n.d.
	H2	0.0	1.3	n.d.	7.3	0.5	n.d.	-12.7	n.d.	n.d.	n.d.	n.d.	n.d.	n.d.	n.d.
	H3	0.0	1.5	0.0	7.4	0.4	n.d.	-12.7	19.2	18.2	n.d.	n.d.	n.d.	n.d.	n.d.
	H4	0.0	1.5	n.d.	7.5	0.6	n.d.	-12.2	n.d.	n.d.	n.d.	n.d.	n.d.	n.d.	n.d.
	H5	0.0	1.2	n.d.	7.3	0.5	n.d.	-12.8	n.d.	n.d.	n.d.	n.d.	n.d.	n.d.	n.d.
	H6	0.0	1.1	0.0	7.3	0.5	n.d.	-12.4	9.6	7.1	n.d.	n.d.	n.d.	n.d.	n.d.
12/09/17	H1	0.0	1.3	0.0	7.1	0.4	n.d.	-12.4	7.0	4.7	3.4	13.5	n.d.	n.d.	n.d.
	H2	0.0	1.2	n.d.	7.5	0.5	n.d.	-12.8	n.d.	n.d.	n.d.	n.d.	n.d.	n.d.	n.d.
	H3	0.0	0.9	0.0	7.1	0.5	n.d.	-12.5	14.9	11.8	3.6	13.8	n.d.	n.d.	n.d.
	H4	0.0	0.8	n.d.	6.5	0.6	n.d.	-12.1	n.d.	n.d.	n.d.	n.d.	n.d.	n.d.	n.d.
	H5	0.0	0.9	n.d.	6.4	0.6	n.d.	-11.8	n.d.	n.d.	n.d.	n.d.	n.d.	n.d.	n.d.
	H6	0.0	1.0	0.0	6.6	0.5	n.d.	-12.0	17.1	13.0	3.1	13.1	n.d.	n.d.	n.d.
02/10/17	H1	0.0	1.4	0.0	7.0	0.4	4.2	-12.7	9.7	8.4	n.d.	n.d.	0.0	0.0	n.d.
	H2	0.1	1.1	n.d.	7.5	0.8	4.2	-11.8	13.7	12.4	n.d.	n.d.	26.5	16.8	n.d.
	H3	0.1	0.4	0.0	8.2	1.3	3.7	-12.1	22.4	20.9	n.d.	n.d.	73.8	43.9	n.d.
	H4	0.2	0.2	n.d.	8.9	1.9	4.5	-11.7	n.d.	n.d.	n.d.	n.d.	87.8	n.d.	n.d.
	H5	0.2	0.2	n.d.	9.1	1.3	4.7	-12.0	n.d.	n.d.	n.d.	n.d.	87.8	n.d.	n.d.

	H6	0.2	0.2	0.0	9.1	2.3	4.4	-13.1	32.9	29.9	n.d.	n.d.	86.3	64.0	78.4
10/10/17	H1	0.0	1.7	0.0	n.d.	0.4	3.7	-12.6	8.5	7.4	3.9	13.9	0.0	0.0	n.d.
	H2	0.0	1.3	n.d.	7.6	0.6	3.7	-12.0	11.7	11.0	n.d.	n.d.	23.8	14.2	n.d.
	H3	0.1	0.5	0.0	8.1	0.9	3.0	-11.4	15.1	14.4	4.3	12.9	72.9	26.6	n.d.
	H4	0.1	0.2	n.d.	8.7	1.6	3.0	-11.1	n.d.	n.d.	n.d.	n.d.	90.7	n.d.	n.d.
	H5	0.1	0.2	n.d.	8.8	1.1	3.9	-11.5	n.d.	n.d.	n.d.	n.d.	89.1	n.d.	n.d.
	H6	0.1	0.2	0.0	n.d.	1.1	3.9	-11.5	34.1	31.9	4.4	12.6	89.5	68.1	100.3
11/05/18	H1	0.0	1.1	0.0	6.9	0.7	3.9	n.d.	11.1	8.0	4.2	12.4	n.d.	n.d.	n.d.
	H2	0.0	1.2	n.d.	7.0	0.7	4.3	n.d.	n.d.	n.d.	n.d.	n.d.	n.d.	n.d.	n.d.
	H3	0.0	1.1	0.0	6.8	0.5	4.2	n.d.	n.d.	n.d.	4.3	12.1	n.d.	n.d.	n.d.
	H4	0.0	1.6	n.d.	0.0	0.5	5.2	n.d.	13.7	11.1	n.d.	n.d.	n.d.	n.d.	n.d.
	H5	0.0	1.3	n.d.	6.9	0.5	5.4	n.d.	13.5	10.7	4.4	12.1	n.d.	n.d.	n.d.
	H6	0.0	1.5	0.0	6.9	0.5	5.4	n.d.	12.7	11.2	n.d.	n.d.	n.d.	n.d.	n.d.
18/05/18	H1	0.0	1.6	0.0	7.1	0.5	5.7	n.d.	12.9	11.9	3.9	12.2	0.0	0.0	n.d.
	H2	0.0	1.5	0.0	7.2	0.6	5.6	n.d.	13.9	10.7	n.d.	n.d.	9.9	0.0	n.d.
	H3	0.1	0.8	0.1	0.0	0.7	5.7	n.d.	20.1	19.0	3.7	12.1	48.0	27.8	n.d.
	H4	0.1	0.2	0.3	8.0	1.3	5.5	n.d.	n.d.	n.d.	n.d.	n.d.	88.8	n.d.	n.d.
	H5	0.1	0.2	0.3	7.9	1.7	5.7	n.d.	32.4	28.2	n.d.	n.d.	88.8	55.8	n.d.
	H6	0.1	0.2	0.1	7.9	1.1	5.5	n.d.	33.9	32.1	3.9	12.2	85.7	61.0	84.5
25/05/18	H1	0.0	1.5	0.0	7.2	0.7	5.8	n.d.	14.0	13.8	3.6	12.4	0.0	0.0	n.d.
	H2	0.0	1.2	0.1	7.5	0.7	5.7	n.d.	11.9	9.5	n.d.	n.d.	21.3	0.0	n.d.
	H3	0.1	0.3	0.0	8.1	1.2	5.3	n.d.	22.4	19.7	4.2	11.8	79.9	27.7	28.1
	H4	0.0	0.0	0.1	9.4	1.6	4.4	n.d.	n.d.	n.d.	n.d.	n.d.	100.0	n.d.	n.d.
	H5	0.1	0.0	0.1	8.1	1.2	5.4	n.d.	n.d.	n.d.	3.9	11.8	100.0	n.d.	n.d.
	H6	0.1	0.0	0.0	8.3	1.0	5.2	n.d.	n.d.	n.d.	n.d.	n.d.	100.0	n.d.	n.d.
12/06/18	H1	0.0	1.2	0.0	0.0	0.8	4.2	n.d.	9.2	7.0	3.9	12.6	0.0	0.0	n.d.
	H2	0.0	1.2	0.0	7.4	0.6	4.3	n.d.	n.d.	n.d.	n.d.	n.d.	5.9	n.d.	n.d.
	H3	0.0	0.9	n.d.	7.3	0.6	4.2	n.d.	10.0	7.1	3.8	12.5	29.4	2.1	n.d.
	H4	0.0	0.8	0.0	0.0	0.6	4.2	n.d.	n.d.	n.d.	n.d.	n.d.	32.1	n.d.	n.d.

Date	Sample														
	H5	0.1	0.8	n.d.	0.0	0.8	4.3	n.d.	n.d.	n.d.	n.d.	n.d.	37.7	n.d.	n.d.
	H6	0.1	0.6	0.0	7.6	0.7	4.3	n.d.	16.3	12.9	3.9	12.4	51.2	25.8	27.1
13/07/18	H1	0.0	1.6	0.0	6.9	0.6	3.5	n.d.	8.4	6.1	n.d.	n.d.	0.0	0.0	n.d.
	H2	0.0	1.5	0.0	6.7	0.7	3.6	n.d.	n.d.	n.d.	n.d.	n.d.	9.7	n.d.	n.d.
	H3	0.0	1.6	0.0	7.1	0.6	3.4	n.d.	9.2	6.6	n.d.	n.d.	2.2	n.d.	n.d.
	H4	0.0	1.4	0.0	0.0	0.6	3.3	n.d.	n.d.	n.d.	n.d.	n.d.	12.0	n.d.	n.d.
	H5	0.1	1.2	n.d.	7.6	0.6	3.3	n.d.	n.d.	n.d.	n.d.	n.d.	27.8	n.d.	n.d.
	H6	0.1	1.0	0.0	0.0	0.6	3.3	n.d.	15.7	12.6	n.d.	n.d.	36.8	26.9	37.4
19/08/18	H1	0.0	1.1	n.d.	0.0	0.8	2.2	n.d.	7.7	5.4	4.7	12.2	0.0	0.0	n.d.
	H3	0.0	1.1	n.d.	0.0	0.6	2.2	n.d.	n.d.	n.d.	4.6	11.9	1.8	n.d.	n.d.
	H4	0.0	1.0	n.d.	7.8	n.d.	2.2	n.d.	n.d.	n.d.	n.d.	n.d.	7.0	n.d.	n.d.
	H5	0.0	1.0	n.d.	n.d.	n.d.	2.1	n.d.	n.d.	n.d.	n.d.	n.d.	4.5	n.d.	n.d.
	H6	0.0	1.0	n.d.	n.d.	0.7	2.1	n.d.	8.8	5.8	4.0	11.8	4.1	3.3	3.1
13/09/18	H1	0.0	1.6	n.d.	n.d.	0.5	2.4	n.d.	7.8	6.7	n.d.	n.d.	0.0	0.0	n.d.
	H2	0.0	1.5	n.d.	n.d.	n.d.	2.5	n.d.	n.d.	n.d.	n.d.	n.d.	5.7	n.d.	n.d.
	H3	0.0	1.3	n.d.	n.d.	0.6	2.5	n.d.	7.6	7.0	n.d.	n.d.	19.0	0.3	n.d.
	H4	0.0	1.3	n.d.	n.d.	n.d.	2.5	n.d.	7.9	10.6	n.d.	n.d.	19.7	8.5	n.d.
	H5	0.0	1.2	n.d.	n.d.	n.d.	2.5	n.d.	n.d.	n.d.	n.d.	n.d.	22.3	n.d.	n.d.
	H6	0.0	1.2	n.d.	n.d.	0.7	2.5	n.d.	9.2	7.6	n.d.	n.d.	24.7	5.0	6.9
19/10/18	H1	0.0	1.6	n.d.	n.d.	0.4	2.6	n.d.	6.7	4.5	n.d.	n.d.	0.0	0.0	n.d.
	H2	0.0	1.7	n.d.	n.d.	n.d.	2.5	n.d.	n.d.	n.d.	n.d.	n.d.	-1.4	n.d.	n.d.
	H3	0.0	0.5	n.d.	n.d.	0.7	2.6	n.d.	7.8	7.1	n.d.	n.d.	68.6	8.3	n.d.
	H4	0.0	1.5	n.d.	n.d.	n.d.	2.6	n.d.	n.d.	n.d.	n.d.	n.d.	8.7	n.d.	n.d.
	H5	0.0	1.5	n.d.	n.d.	n.d.	2.6	n.d.	n.d.	n.d.	n.d.	n.d.	6.6	n.d.	n.d.
	H6	0.0	1.4	n.d.	n.d.	0.4	2.6	n.d.	11.4	10.1	n.d.	n.d.	12.6	21.0	29.4

X^1 is calculated from concentration data while X^2 is calculated from isotopic data

n.d. = non determined

NH_4^+ in the 2017 campaigns was analyzed by ion chromatography while in the 2018 campaigns by ion selective electrode